The role of Kupffer cells in mediating the microcirculatory and biochemical consequences of endotoxemia and obstructive jaundice in rats

Ph.D. Thesis

Szabolcs Ábrahám, MD

Department of Surgery
Faculty of Medicine, University of Szeged
Szeged, Hungary

2009

CONTENTS

List of full papers related to the subject of the thesis:

I. **Ábrahám S**, Szabó A, Kaszaki J, Varga R, Eder K, Duda E, Lázár G, Tiszlavicz L, Boros M, Lázár G Jr. Kupffer cell blockade improves the endotoxin-induced microcirculatory inflammatory response in obstructive jaundice. *Shock* 30: 69-74, 2008.

II. **Ábrahám S**, Szabó A, Paszt A, Duda E, Lázár G, Lázár G ifj: A Kupffer-sejt gátlás hatása az endotoxin indukálta gyulladásos válaszreakciókra és a máj mikrokeringési változásaira kísérletes obstrukciós icterusban. *Magyar Sebészet* 2009 (accepted, in press).

III. **Ábrahám S**, Hermesz E, Szabó A, Ferencz A, Duda E, Ábrahám M, Lázár G, Lázár G Jr. The effects of Kupffer cell blockade on the hepatic expression of metallothionein and heme oxygenase genes in endotoxemic rats with obstructive jaundice (submitted for publication).

List of abstracts related to the subject of the thesis:

I. **Ábrahám S**, Szabó A, Lázár G, Lázár G Jr. Kupffer cell blockade ameliorates the obstructive jaundice-induced microcirculatory inflammatory reaction in the liver. *European Surgical Research* 28: 1-124, 2005.

II. **Ábrahám S**, Ferencz A, Szabó A, Lázár G, Boros M, Hermesz E, Lázár G Jr. Hepatic expression and regulation of metallothionein and heme oxygenase genes in endotoxemic rats with obstructive jaundice – the role of Kupffer cells. *European Surgical Research* 39: 1-90, 2007.

III. Lázár G Jr, **Ábrahám S**, Szabó A, Kaszaki J, Duda E, Lázár G, Tiszlavicz L, Boros M. Kupffer cell blockade improves the endotoxin-induced microcirculatory inflammatory response in obstructive jaundice. *Shock* 29 Suppl 1, 2008.

IV. **Ábrahám S**, Hermesz E, Ferencz A, Szabó A, Lázár G, Boros M, Lázár G Jr. Antioxidant defense system in endotoxemic rats with obstructive jaundice. *Shock* 29 Suppl 1, 2008.

List of abbreviations:

BDL	bile duct ligation
CAT	catalase
ET-1	endothelin-1
$GdCl_3$	gadolinium chloride
HO	heme oxygenase
IL-6	interleukin-6
IVM	intravital microscopy
KC	Kupffer cell
LPO	lipid peroxidation
LPS	lipopolysaccharide
MPO	myeloperoxidase
MT	metallothionein
PMN	polymorphonuclear leukocytes
RES	reticuloendothelial system
SOD	superoxide dismutase
TNF-α	tumor necrosis factor alpha
TXA	thromboxane

1. INTRODUCTION

1.1. Septic complications of obstructive jaundice

Patients with obstructive jaundice undergoing surgical procedures have a significant risk of complications and death (Greig JD, 1988; Lai LC, 1992). Gram-negative sepsis constitutes the bulk of the morbidity and mortality, although renal dysfunctions, coagulopathy, gastrointestinal hemorrhage and impaired wound healing are also well recognized (Armstrong CP, 1984).

Clinical and experimental studies have suggested several etiological factors for these complications, including hypotension, an impaired nutritional status, an impaired immune function and the presence of potential toxic substances in the circulation, such as bilirubin and bile acids (Pitt HA, 1981; Oh HC, 2007). However, in recent years, there has been an increasing recognition of the role of circulating endotoxins in the development of complications in obstructive jaundice (Diamond T, 1991). Many authors, using a variety of clinical and biochemical parameters, have attempted to identify those jaundiced patients most at risk; neverless, there has been no universally accepted theory for the pathophysiology of the complications seen in biliary obstruction (Blamey SL, 1983; Lacaine F, 1995)

In surgical practice, biliary obstruction is often combined with septic complications. A microcirculatory dysfunction and leukocyte activation are interdependent components of acute liver injuries, including lipopolysaccharide (LPS)-induced hepatic damage. Intrahepatic leukocyte activation and microvascular perfusion failure are also involved in the pathology of biliary obstruction (Koeppel TA, 1997; Ito Y, 2000; Ito Y, 2003). The precise mechanisms that participate in the susceptibility of jaundiced patients to sepsis, however, are still unclear and the relative impact of an increased LPS load on a cholestatic microcirculatory dysfunction is as yet undefined. Gram-negative sepsis and its sequelae occur frequently in patients with extrahapatic obstructive jaundice following invasive diagnostic or therapeutic procedures. Normally, small quantities of endotoxin in the portal circulation are cleared by Kupffer cells (KCs) (Carrico CJ, 1993).

We therefore applied clinically relevant models of obstructive jaundice in combination with endotoxemia in rats, in order to test whether the microcirculatory and biochemical consequences of bile duct ligation (BDL) are deteriorated by an additional LPS challenge.

1.2. The role of Kupffer cells in different inflammatory processes

The liver KCs comprise the largest macrophage population in the human organism. KCs, resident liver macrophages, constitute 80-90 per cent of the fixed-tissue mononuclear cell population. They are positioned at the interface between the portal and systemic circulations and are responsible for sequestering pathogenic substances, including bacteria and toxins, from the portal circulation (Jacob AI, 1977). The KCs of the hepatic reticuloendothelial system (RES) synthesize and secrete various bioactive compounds, including reactive oxygen and nitrogen radicals, eicosanoids and peptide mediators, forming the first line of defense against microorganisms entering the portal circulation (Crofton RW, 1978). KC activation and the subsequent secretion of inflammatory mediators are fundamental for an effective immune response. Persistently high or overwhelming activation may result in an uncontrolled initiation of the proinflammatory cascade, leading to the systemic inflammatory response syndrome and potentially to the multiple organ dysfunction syndrome (Carrico CJ, 1993).

Mediating an appropriate immune response, KC activation is likely to play protective roles in the acute phase of hepatic pathologies (Gehring S, 2006). However, in response to an ongoing bacterial or endotoxin challenge, KC activation may increase the severity of the liver dysfunction (Barriault C, 1995). In LPS-induced sepsis, KCs eliminate LPS and other agents primarily from the portal blood, protecting the hepatocytes from exposure to high levels of LPS and other oxidative stresses. However, it is believed that LPS-stimulated KCs produce tumor necrosis factor-alpha (TNF-α), resulting in hepatocyte and endothelial damage, indicating that activation of the KCs is responsible for liver damage (Van Bossuyt H, 1988; Naito M, 2004).

In experimental biliary obstruction models, an enhanced susceptibility of jaundiced animals to endotoxemia has been demonstrated, which was critically linked to the activation of KCs (Lázár G Jr, 2002; Minter RM, 2005). The KC functions are altered after biliary obstruction (O'Neil S, 1997; Harry D, 1999; Kennedy JA, 1999), the KC-dependent immune modulation then possibly leading to divergent outcomes (Katz S, 1984; Ball SK, 1991; Ding JW, 1992; Tomioka M, 2000). Defects in crucial elements of the function of the RES after cholestasis lead to hypersensitivity to LPS, with a high rate of septic complications in the long run (O'Neil S, 1997; Harry D, 1999; Kennedy JA, 1999;). Most of the above reactions and

also the production of the proinflammatory cytokines were enhanced when obstructive jaundice was followed by a second hit of LPS (Busam KJ, 1990; Hoffmann R, 1994), and biliary obstruction exacerbates the hepatic microvascular inflammatory response to endotoxin (Ito Y, 2000).

Macrophage blockade has the theoretical advantage of abrogating inflammatory responses at an earlier stage of sepsis. Rare earth metal salts, including gadolinium chloride ($GdCl_3$) depress the RES activity (Lázár G, 1973) and selectively interfere with the function of the KCs. $GdCl_3$ inhibits the secretion of biologically active substances from the liver KCs, and the liver-damaging effects of hepatotoxins (Barriault C, 1995), ischemia reperfusion (Giakoustidis DE 2003; Jung JY, 2005) and the develpoment of septic shock (Lázár G Jr, 1987). However, it has been demonstrated that attenuation of the KC activity with $GdCl_3$ might decrease the LPS-induced lethality and morbidity in obstructive jaundice (Lázár G Jr, 2002; Minter RM, 2005). In the present studies, we also applied this compound as a 24-h pretreatment in the different models (during BDL with or without endotoxemia). During our examinations, we also wanted to test the possible side-effects of this treatment (see Lázár G Jr, 2002). We hypothesized that a change in the level of activation of the KCs would be a significant determinant factor in the pathomechanism of the inflammatory consequences of obstructive jaundice.

1.3. The role of leukocytes in various inflammatory processes in the liver

Endotoxemia/sepsis induces an inflammatory response, with the leukocytes primarily contributing to hepatocellular injury by the release of a variety of mediators. Although, in turn, necessary for vital host defense mechanisms, leukocytes can considerably aggravate tissue injury. Previously, the intrasinusoidal sequestration of leukocytes with transmigration into the tissues has been identified as a critical step of endotoxin-induced liver injury. After transmigration, the neutrophils attack the parenchymal cells and cause severe liver cell necrosis. Within this process, apoptotic hepatocytes have been shown to function as chemotactic signals, triggering leukocyte transmigration and thereby sustaining the cell-dependent inflammatory response (Chosay JG, 1997; Lawson JA, 1998).

Investigations utilizing intravital microscopy (IVM) have demonstrated that the recruitment of inflammatory cells into the perivascular tissue involves a complex cascade

mechanism. The adhesion process consists of several steps, beginning with the rolling of polymorphonuclear leukocytes (PMNs) on the endothelial surface of the postcapillary venules until they have slowed down to such a degree that they stick to the endothelium. At this point, the leukocytes are sequestered from the main vascular flow, and firm adherence to the endothelial cells may follow. Subsequently, the leukocytes pass an intercellular junction between the endothelial cells and reach the abluminal side.

Three families of leukocyte-endothelial adhesion molecules have been identified: the selectins, the immunoglobulin gene superfamily, and the integrins. The selectin family comprises three proteins, designated by the prefixes L (leukocyte), P (platelet) and E (endothelial). This is a class of cell adhesion molecules which mediate leukocyte rolling on the endothelium. P-Selectin (CD62P), which is stored in the Weibel-Palade bodies of the endothelial cells, is rapidly mobilized to the plasma membrane in response to proinflammatory mediators such as thrombin or histamine (Bonfanti R, 1989; Lorant DE, 1991). L-Selectin (CD62L) is expressed on most types of leukocytes and is shed from the cell membrane by proteolytic cleavage after cellular activation. E-Selectin (CD62E), which is not expressed on the endothelial cell membrane under basal conditions, is synthesized after stimulation by inflammatory mediators such as TNF-α and endotoxin (Eppihimer MJ, 1996). After the leukocyte has been arrested, integrins are activated by chemokines, chemoattractants and cytokines. During the transmigration process, a vascular dysfunction may occur due to the inappropriate release of oxidants, proteases and other potent mediators of the activated leukocytes.

We used IVM to observe the microcirculatory consequences of the above challenges directly in the liver. This method provided a possibility for the nearly online quantification of hepatic perfusion changes and of the primary and secondary PMN-endothelial interactions. Furthermore, this tool enabled us to quantify the hepatic activation of KCs.

1.4. The role of free radicals in sepsis and organ injury

The mechanisms involved in shock and organ injury induced in septic shock are multifactorial. Diverse molecular mechanisms of inflammation and cellular damage have been implicated in the pathogenesis of septic shock and multiple organ failure, including those related to the overt generation of cytokines, eicosanoids and reactive oxygen species, such as

nitric oxide, superoxide anion or peroxynitrite (Gutteridge JM 1995). Under normal physiological conditions, the majority of reactive oxygen species are formed during cellular respiration and by activated phagocytic cells, including PMNs and KCs, and a homeostatic balance exists between the formation of reactive oxidizing/oxygen species and their removal by endogenous antioxidant scavenging compounds. Oxidative stress occurs when this balance is disrupted by the excessive production of oxygen and nitrogen-derived free radicals, and/or by inadequate anti-oxidative defense mechanisms. As a result, oxidation of DNA and proteins may take place, along with membrane damage because of lipid peroxidation (LPO), leading to alterations in membrane permeability, modification of protein structure and functional changes (Zimmerman JJ, 1995).

The most efficient enzymatic antioxidants involve superoxide dismutase (SOD), catalase (CAT) and glutathione peroxidase (for a review see, Sakaguchi S, 2006). SOD is a highly effective intracellular enzymatic antioxidant which catalyzes the dismutation of $O_2^{\bullet -}$ to oxygen and to the less-reactive species hydrogen peroxide by catalyzing the dismutation of the superoxide anion to oxygen and water. (McCord JM, 1969). There are three forms of SOD: cytosolic Cu/Zn-SOD, mitochondrial Mn-SOD and extracellular SOD (Fridovich I, 1995). CAT is located in a cell organelle called the peroxisome. The enzyme very efficiently promotes the conversion of hydrogen peroxide to water and molecular oxygen. CAT has one of the highest turnover rates for all enzymes: one molecule of CAT can convert 6 million molecules of hydrogen peroxide to water and oxygen each minute (Matés JM, 1999).

1.5. Heme oxygenase and metallothioneins as special components of the antioxidant defense system

Tissue damage resulting from endotoxemia or obstructive jaundice also leads to the activation of endogenous protective mechanisms. Among the upregulated proteins, the expression of the microsomal enzyme heme oxygenase (HO) is triggered by both endotoxemia and biliary obstruction (Bauer I, 1998; Froh M 2007). HO plays role a in heme degradation, and also produces carbon monoxide, a vasoactive dilalator agent with important free radical scavenger properties (Gemsa D, 1974; Stocker R, 1990; Camhi SL, 1995). The fact that stress reactions, including endotoxemia, are associated with HO upregulation in the KCs, suggests that these self-defensive anti-inflammatory reactions are also initiated in this

important proinflammatory cellular component of the liver (Gemsa D, 1974; Stocker R, 1990; Rizzardini M, 1994).

There are also other, albeit not enzymatic proteins in the liver with metal-binding and considerable anti-inflammatory properties. Metallothioneins (MTs) are low molecular weight, non-enzymatic proteins that play a homeostatic role in the control and detoxification of the heavy metals. MTs are constitutively expressed in the liver and are overexpressed in endotoxemia (Abe S, 1987; Kille P, 1994; Hur T, 1999). As one-third of its amino-acid residues are cysteines, MT provides a neutrophilic sink binding electrophiles (Kojima Y, 1976; Kille P, 1994). MTs may ameliorate the effects of oxidative stress by scavenging free radicals (Sato M, 1993) and even by preventing their formation (Takano H, 2004).

The purpose of the second part of the study was to examine the effects of endotoxemia with or without biliary obstruction on hepatocellular damage, on the endogenous antioxidant mechanisms, and on the HO and MT expression changes, by using molecular biological methods. Furthermore, we wanted to elucidate the effects of the KC blockade with $GdCl_3$ on these parameters.

2. AIMS

The aims of the present study were:

1. To evaluate the hepatic inflammatory consequences of 3-day obstructive jaundice in the presence and absence of acute endotoxemia:

- By examining the early inflammatory complications of obstructive jaundice with *in vivo* microscopic methods. With this aim, we performed experiments to characterize the inflammatory microvascular alterations (hepatic microvascular perfusion and leukocyte-endothelial interactions).
- By quantification of the accumulation of neutrophilic leukocytes by means of hepatic myeloperoxidase (MPO) activity measurements.
- By assessing the expression changes in proinflammatory cytokine (interleukin-6 (IL-6) and TNF-α) release.

- By characterizing the isoform-specific HO and MT gene induction changes.
- By examining the functional and structural indices of liver injury, oxidative hepatic injury (DNA damage and lipid peroxidation) and histological liver injury.
- By assessing the changes in activity of the different components of the endogenous anti-oxidant defense system (CAT and Mn- and Cu/Zn-SOD) during the above challenges.

2. To examine the activation of KCs by using an IVM approach and to assess their role in the above changes by inhibition of the KC function with 24-h $GdCl_3$ pretreatment.

3. MATERIALS AND METHODS

The experiments were performed in adherence to the National Institutes of Health guidelines for the use of experimental animals. The study was approved by the Ethical Committee for the Protection of Animals in Scientific Research at the University of Szeged.

Animals

Male outbred Wistar rats from the University of Szeged (weighing 250-300 g) were maintained on standard laboratory diet and tap water *ad libitum* and housed in an environmentally controlled room under a 12-h light - 12-h dark cycle.

3.1. Experimental protocol and experimental groups

Two major experimental series were performed. In the first series, the animals were allocated randomly to one or other of four groups (Figure 1). In the first group, endotoxemia was elicited by injecting a low dose (1 mg/kg bw) of LPS (*E. coli* 026:B6 LPS B. Difco; Laboratories, Detroit, MI, USA) i.v. through the tail vein, 2 h before the IVM measurements (LPS group, n=5). In another group, extrahepatic biliary obstruction was induced by BDL 3 days prior to the measurements (BDL group, n=5). Briefly, a short midline abdominal incision was made and the common bile duct was ligated with a 4-0 silk suture under light oxygen-ether anesthesia. The abdomen was then closed in two layers and the animals were allowed to recover. In a third group, these challenges were combined (BDL + LPS group).

The data were compared with those on sham-operated animals (Sham group, *n*=5). The animals in all groups received 1 ml/kg saline i.v. through the tail vein 24 h before the examinations.

After characterization of the consequences of the above major challenges, additional experimental groups were used to examine the effects of KC blockade (Series 2). In this series, the rats were pretreated with $GdCl_3$ (10 mg/kg bw i.v. through the tail vein; Prolabo, Paris, France) (Lázár G, 1973; Husztik E, 1980) 24 h before the IVM examinations; the animals were then challenged with the sham operation (Sham + $GdCl_3$ group, *n*=5), with BDL (BDL + $GdCl_3$ group, *n*=5), with LPS (LPS + $GdCl_3$ group, *n*=5) or with their combination (BDL + LPS + $GdCl_3$ group, *n*=5). At the end of the experiments, blood samples for proinflammatory serum cytokine (TNF-α and IL-6) assessment and liver biopsies for biochemical and histological evaluations (see later) were taken.

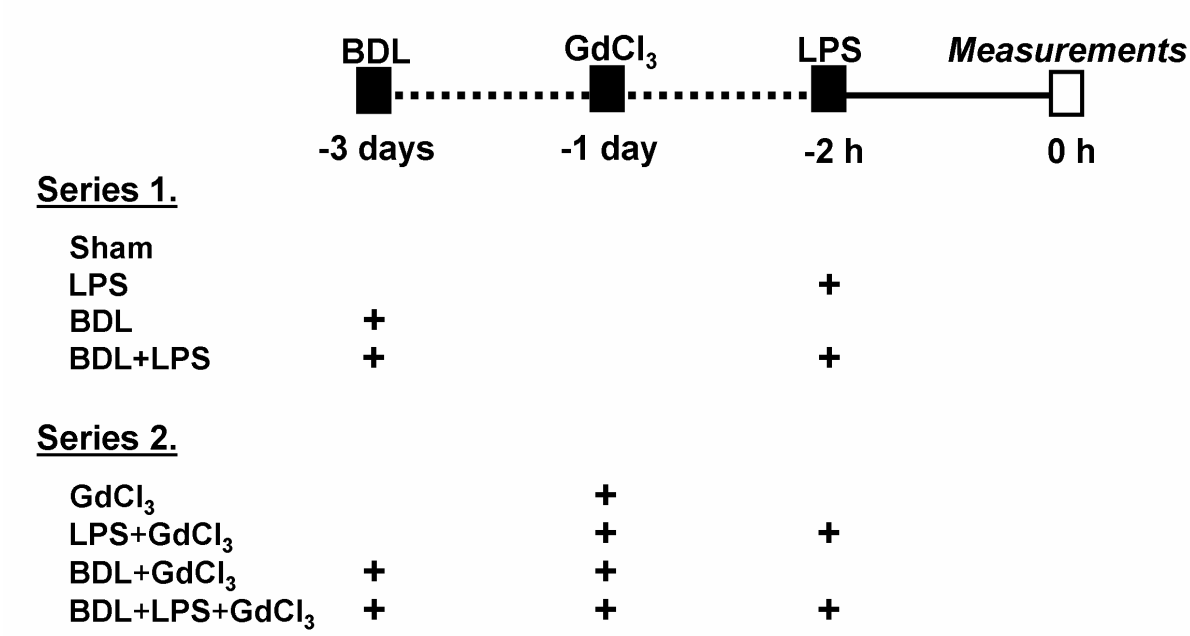

Figure 1. Experimental series and groups. Sham-operated animals served as controls (*n=5*); in the LPS group, endotoxemia was elicited by injecting a low dose of *E.coli* LPS iv. 2 h before the examinations (*n=5*); in the BDL group, extrahepatic BDL was induced 3 days prior to measurements (*n=5*); in the BDL+LPS group, the previous challenges were combined (*n=5*); In the second series, the same experiments were repeated in four groups of rats (*n=5*, each), but these animals were pretreated with $GdCl_3$ (1 mg/100 g bw) i.v. 24 h before the experiments.

3.2. Microcirculatory parameters

3.2.1. Intravital fluorescence microscopy of the liver

For the IVM examinations, animals were anesthetized with sodium pentobarbital (45 mg/kg i.p.), placed in the supine position on a heating pad (the body temperature was kept at 36-37 °C) and tracheotomized to facilitate spontaneous respiration. Polyethylene catheters placed in the right carotid artery and jugular vein allowed for the monitoring of the systemic hemodynamics (mean arterial pressure and heart rate), blood sampling and injections of fluorescent dyes for IVM. Following a transverse subcostal laparotomy, the left liver lobe was exteriorized, placed on a specially designed pedestal, and covered with a glass slide and a heating pad, turned on its left side, providing a suitable horizontal plane of the liver lobe for intravital microscopic examinations (McCuskey RS, 1993; Vollmar B, 1993).

The hepatic microcirculation was analyzed by means of an epi-illumination technique, using a fluorescence videomicroscope (Zeiss Axiotech Vario 100HD supplied with a 100 W HBO mercury lamp and an Acroplan 20x water immersion objective) with a blue (450-490/>515 nm) and a green (525-555/>580 nm) filter system. The microscopic images were recorded by a charge-coupled device video camera (AVT HORN-BC 12) attached to a video system (Panasonic AG-MD 830). The contrast enhancement was achieved by injecting sodium fluorescein (75 μg/kg i.v., Sigma, St. Louis, MO, USA). Leukocytes were stained *in vivo* by means of rhodamine-6G (0.2%, 0.1 ml i.v., Sigma, St. Louis, MO, USA). For the IVM analysis of KC phagocytic activity, plain fluorescent latex particles (diameter 1.0 μm; Polysciences Inc., Warrington, PA, USA) were injected i.v. ($3x10^8$/ml/kg sterile isotonic saline as a bolus injection).

At the end of the 30-min observation period, plasma samples (for IL-6 and TNF measurements) and liver biopsies (for biochemical and histological evaluations) were taken and the animals were killed with an overdose of pentobarbital.

3.2.2. Video analysis

Capillary perfusion, leukocyte-endothelial interactions and KC activity were quantified off-line, using computer-assisted analysis of the video recordings (IVM Software, Pictron Ltd., Budapest, Hungary).

The *microcirculatory perfusion failure* was quantified by calculating the ratio of perfused and non-perfused capillaries within 10 acini per animal. *Leukocyte-endothelial interactions* were described by calculating the number of sticking leukocytes within 5 central venules per animal. A leukocyte was defined as firmly adherent if it remained stationary for at least 30 s. The number of leukocytes sticking to the endothelial surface (mm^2) was calculated from the diameter and length of the vessel segment, assuming cylindrical geometry. *The phagocytic function of the hepatic macrophages* was assessed by measuring the phagocytosis of fluorescent 1.0 µm latex particles by individual cells. The number of macrophages was measured via the number of phagocyted latex microspheres within 10 acini in each animal 20 min after injections of the microbeads (Vollmar B, 1996).

3.3. Biochemical parameters

3.3.1. Myeloperoxidase activity

The tissue MPO activity, as a marker of tissue leukocyte infiltration, was measured in liver biopsies by the method of Kuebler *et al.* (Kuebler WM, 1996). Briefly, the tissue was homogenized with Tris-HCl buffer (0.1 M, pH 7.4) containing 0.1 mM polymethylsulfonyl fluoride to block tissue proteases, and then centrifuged at 4 °C for 20 min at 2000g. The MPO activities of the samples were measured at 450 nm (UV-1601 spectrophotometer, Shimadzu, Japan), and the data were referred to the protein content.

3.3.2. Cytokine assays

TNF-α cytotoxicity was measured by standard procedures, using mouse WC-1 tumor cells in the presence of 1 µg/ml actinomycin-D at 37 °C (Aggarwal BB, 1985). Cell killing was assessed by the reduction of 3-(4,5-dimethylthiazol-2-yl)-2,5-diphenyltetrazolium bromide. The amount of TNF-α required to mediate the half-maximum cytotoxicity of WC-1 cells was assigned as 1 unit (U).

IL-6 was measured via the degree of proliferation of a murine hybridoma cell line (B9), which grows only in the presence of IL-6. The proliferation of the hybridoma cells stimulated with serum was determined by 3-(4,5-dimethylthiazol-2-yl)-2,5-diphenyltetrazolium bromide assay after an incubation period of 72 h. All samples in the assays were tested in duplicate.

3.3.3. RNA extraction, reverse transcription and PCR amplification

For molecular biological examinations, the liver tissues were removed, frozen immediately in liquid nitrogen and stored at –80 °C. Approximately 100 mg of frozen tissue was homogenized in RNAzol B reagent (Tel-Test, Inc., Friendswood, TX, USA) and the total RNA was prepared according to the procedure suggested by the manufacturer. The total RNA was routinely treated with 100 U of RNAse-free DNAse I to avoid any DNA contamination. To quantify MT and HO-specific mRNAs, an RT-PCR-based strategy was employed. First-strand cDNA was synthetized by using 5 μg total RNA as template. The RNA was denatured at 90 °C, and mixed with 200 pmol of each dNTP (Sigma, St. Louis, MO, USA), 200 U of M-MuLV reverse transcriptase (Sigma, St. Louis, MO, USA) and 500 pmol of random hexamer primer. The reaction mixture was incubated for 10 min at 37 °C, followed by 1 h at 42 °C. The reaction was stopped by heating at 65 °C for 5 min. 2 μl of reverse transcription product was added to 48 μl of PCR reaction mixture containing 250 μmol of each dNTP, 1x Sigma PCR buffer/$MgCl_2$, 5 U of Taq polymerase (Sigma St. Louis, MO, USA) and 50 pmol of primers specific to the MT-1, MT-2 and HO-1 and HO-2 isoforms and the β-actin gene. Amplification was performed in a PTC 200 Peltier Thermal Cycler (MJ Research, Waltham, MA, USA). The number of amplification cycles during which PCR product formation was limited by the template concentration was determined in pilot experiments: for β-actin 25, and for MTs and HOs 30 cycles were used. The amplified products were electrophoresed on 2% agarose (Sigma, St. Louis, MO, USA) gel.

3.3.4. Primers and measurement of metallothionein and heme oxygenase mRNA levels

For the amplification of rat MT and HO mRNAs, isoform-specific primers were designed on the basis of the databank entries M11794 and AY341880 for the MT-1/2 isoforms, and NM_012580 and NM_024387 for the HO-1/2 isoforms. For normalization of the amounts of MT and HO mRNAs, the β-actin mRNA level was used as internal standard. The sequences of the primers β-actin-3 and 4 were derived from GeneBank entry M24113. Images of ethidium bromide-stained agarose gels were digitalized with a GDS 7500 Gel Documentation System and analyzed with GelBase/GelBlot™ Pro Gel Analysis Software (UVP Inc., San Gabriel, CA, USA). The relative levels of MT and HO mRNAs are expressed

as the ratio MT/β-actin or HO/β-actin. For each experimental treatment, 5 animals were used to prepare RNA. RT-PCR reactions for each animal were performed in triplicate to increase the reliability of the measurements.

MT-1 F: 5'ATGGACCCCAACTGCTCCTG 3',
MT-1 R: 5'TGGAGGTGTACGGCAAGACT 3',
MT-2 F: 5'AACTGCTCCTGTGCCACAGG 3',
MT-2 R: 5'GAAAAAAGTGTGGAGAACCG 3',
HO-1 F: 5' TGGGCTCCCTATACCAGATC 3',
HO-1 R: 5' ATGCCCTTCTTCCAGTGGGG 3',
HO-2 F: 5' TTTTAAGCTTGCCACCACTG 3',
HO-2 R: 5' CCTGGTTCTCCCAGTCTTCA 3',
β-actin-3: 5' GCAAGAGAGGTATCCTGACC 3',
β-actin-4: 5' CCCTCGTAGATGGGCACAGT 3'.

3.3.5. Catalase activity

CAT activity was determined spectrophotometrically at 240 nm by the method of Beers *et al*. (Beers RF Jr, 1952) and expressed in Bergmeyer units (BU) (1 BU = decomposition of 1 g H_2O_2/min at 25 °C).

3.3.6. Superoxide dismutase activity

SOD activity was determined on the basis of the inhibition of epinephrine-adrenochrome autoxidation (Beauchamp C, 1971; Misra HP, 1972). Mn-SOD activity was measured by the autoxidation method in the presence of 5×10^{-3} M KCN. Cu/Zn-SOD activity was calculated by deduction of the Mn-SOD activity from the total SOD activity.

3.3.7. Lipid peroxidation

LPO was estimated from the formation of thiobarbituric acid-reactive substances, determined by using a modification of a method described by Serbinova *et al*. (Serbinova E, 1992) and expressed as nanomoles per gram of wet tissue.

3.3.8. DNA single-strand breaks

The alkaline fluorescence analysis of DNA unwinding was used to determine single-strand DNA breaks. DNA samples were prepared from the livers of control and treated animals by using the salting-out method of Miller *et al*. (Miller SA, 1988). To quantify undamaged double-stranded DNA, samples were divided into three sets (F, F_{min} and F_{max}) and the DNA fluorescence was determined under different conditions. To measure F values, the DNA was kept at pH 12.4 to permit its partial unwinding. To determine F_{min}, the DNA samples were kept at pH 12.4, but before the incubation period, they were sonicated for 1 min. For F_{max} determination, the DNA samples were kept at pH 10, which is below the pH needed to induce the unwinding of the DNA. Samples were incubated on ice for 30 min, followed by a 15-min incubation at 15 °C. Fluorescence was measured after the addition of ethidium bromide at 0.67 μg/ml, with an excitation wavelength of 520 nm and an emission wavelength of 590 nm. The results are expressed as D (percentage of double-stranded DNA) = $(F- F_{min})/ (F- F_{max})$ x 100.

3.4. Histology

Tissue specimens from livers were fixed in 10% buffered formalin and embedded in paraffin. Representative tissue sections were cut (6 μm) from paraffin blocks and stained with hematoxylin and eosin for light microscopy. Histological analysis and the scoring of damage were performed in coded sections by a skilled histologist. Portal, periportal and intralobular evaluations were used to quantify the degree of damage, using a 0-5 grade damage scoring system. Measures of portal damage included chronic inflammation (inflammatory cell infiltration), bile duct proliferation and fibrosis. Periportal damage was quantified by the degree of acute cholangiohepatitis and piecemeal necrosis. Intralobular changes included focal necrosis/apoptosis, zonal/multiacinar necrosis and KC hypertrophy.

3.5. Statistical analysis

Data in all Figures are expressed as means ± standard error of the mean (SEM). Data analysis was performed with a statistical software package: SigmaStat version 3.1 (Jandel

Corporation, San Rafael, CA, USA). Changes in variables within and between groups were analyzed by two-way ANOVA followed by the Holm-Sidak test. *P* values < 0.05 were considered statistically significant.

4. RESULTS

The baseline values of mean arterial pressure did not differ significantly in the different groups, and there were no significant changes in this parameter during the course of the experiments in any of the groups examined. This was not influenced by the $GdCl_3$ treatment either (data not shown).

4.1. Microcirculatory changes

4.1.1. Changes in microcirculatory liver perfusion

In response to BDL, significantly lower rates of perfused capillaries were found (approximately 63%) than in the sham-operated animals (approximately 89%) (Figure 2). Furthermore, the perfusion failure caused by BDL was greatly potentiated by the LPS challenge, whereas the rate of the perfused capillaries did not reach 50%. A slightly ameliorated hepatic capillary perfusion failure in response to KC blockade by $GdCl_3$ pretreatment was found in the BDL + LPS group.

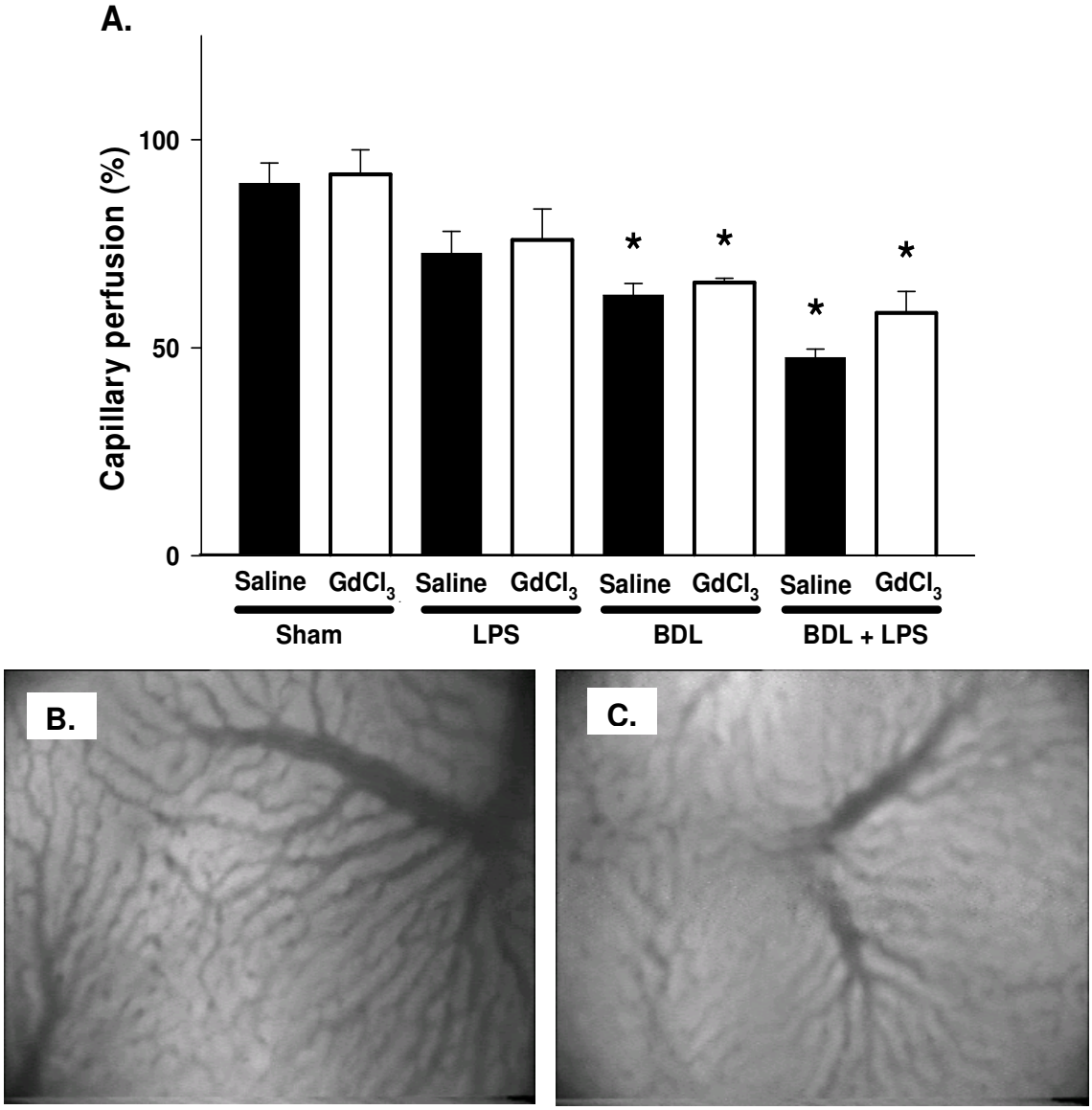

Figure 2. Changes in the capillary perfusion (A) in response to sham operation (Sham), endotoxemia induced with LPS, BDL or BDL + LPS (black bars), and the effects of $GdCl_3$ pretreatment (white bars). Data are presented as means ± SEM. * $P < 0.05$ *vs* Sham. Representative IVM images of the liver in response to Sham (B) and BDL (C).

4.1.2. Changes in leukocyte adherence in the central venules of the liver

Significantly higher numbers of firmly adherent leukocytes in the central venules were found after LPS (approximately 5-fold) and BDL + LPS (approximately 6-fold) in comparison with those in the sham-operated group. These changes were completely abolished by $GdCl_3$ in the LPS group and significantly ameliorated in the animals challenged with BDL + LPS (Figure 3).

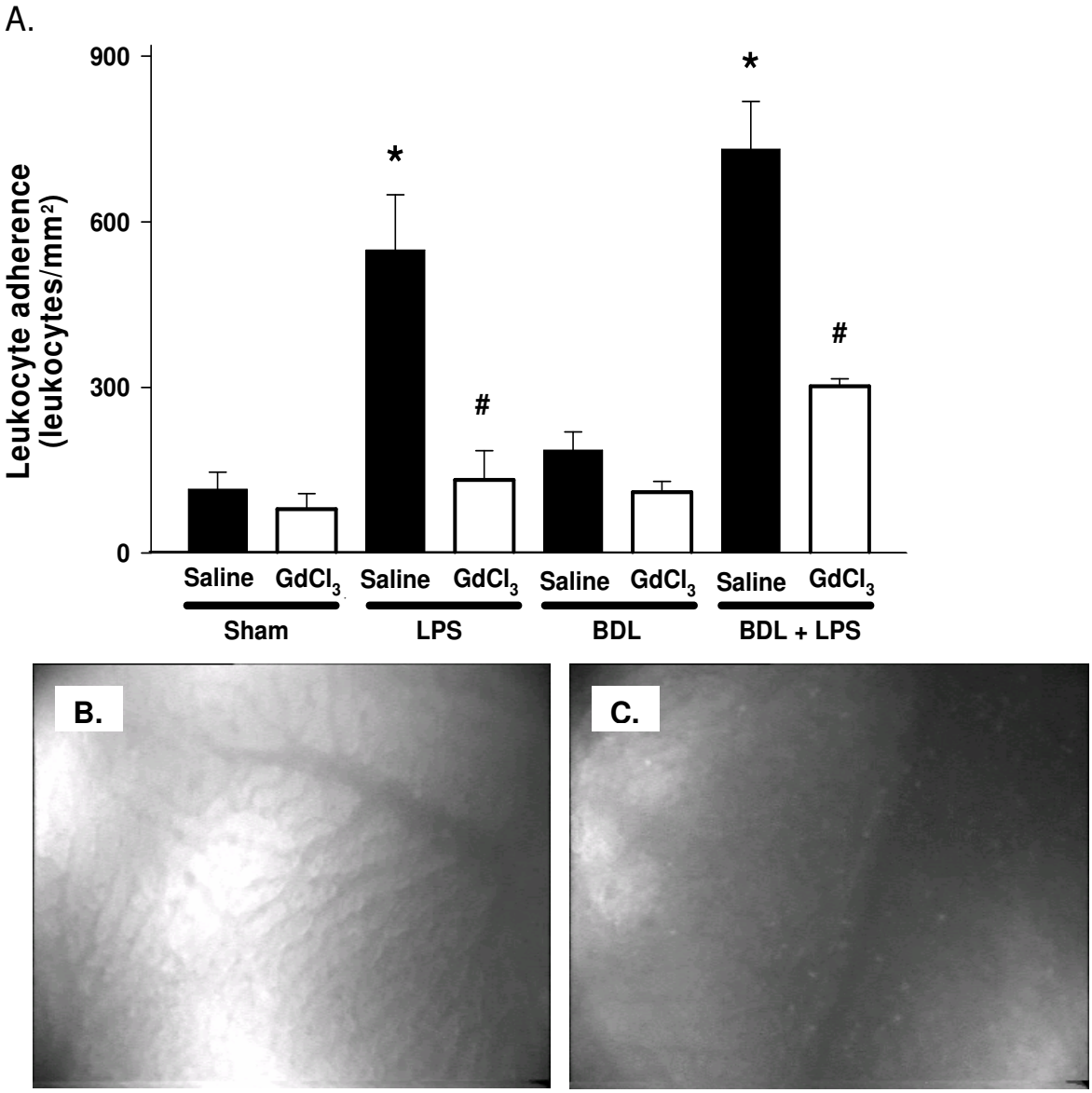

Figure 3. Changes in leukocyte adhesion to the central venular endothelium in response to sham operation (Sham), endotoxemia induced with LPS, BDL or BDL + LPS (black bars), and the effects of $GdCl_3$ pretreatment (white bars). Data are presented as means ± SEM. * $P < 0.05$ *vs* Sham; # $P < 0.05$ *vs* Saline. Representative IVM images of the liver in response to Sham (B) and LPS (C).

4.1.3. Changes in Kupffer cell activation in the liver

The phagocytic activity of the KCs was estimated via the number of phagocytosed latex microspheres (Figure 4). These values were approximately 3-fold higher in the BDL and LPS-treated animals, and approximately 5-fold higher in the combined group, in comparison with the shams. These changes were reduced by $GdCl_3$ treatment in each of the above groups.

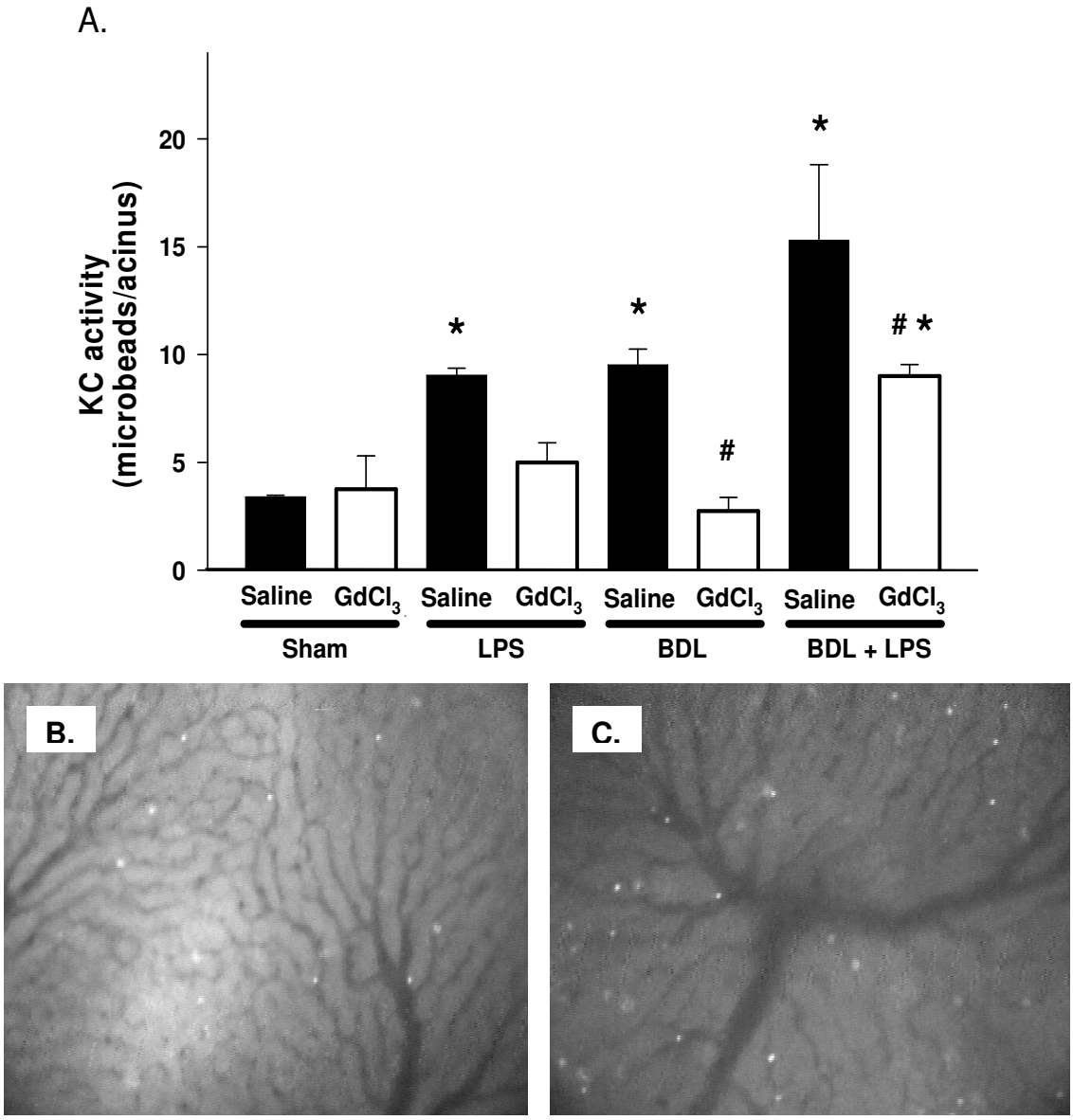

Figure 4. Effects of $GdCl_3$ pretreatment on the KC activity (A) in response to sham operation (Sham), endotoxemia induced with LPS, BDL or BDL + LPS (black bars), and the effects of $GdCl_3$ pretreatment (white bars). Data are presented as means ± SEM. * $P < 0.05$ *vs* Sham; # $P < 0.05$ *vs* Saline. Representative IVM images of the liver after injection with fluorescent latex particles for the assessment of KC phagocytic activity in control (Sham, B) and BDL+LPS-challenged animals.

4.2. Biochemical changes

4.2.1. Changes in leukocyte accumulation in the liver

As evidenced by the MPO measurements (Figure 5), obstructive jaundice caused a moderate, while LPS induced a marked leukocyte accumulation in the liver, which was

greatly augmented when these challenges were combined. In this latter group, $GdCl_3$ significantly attenuated PMN deposition in the liver.

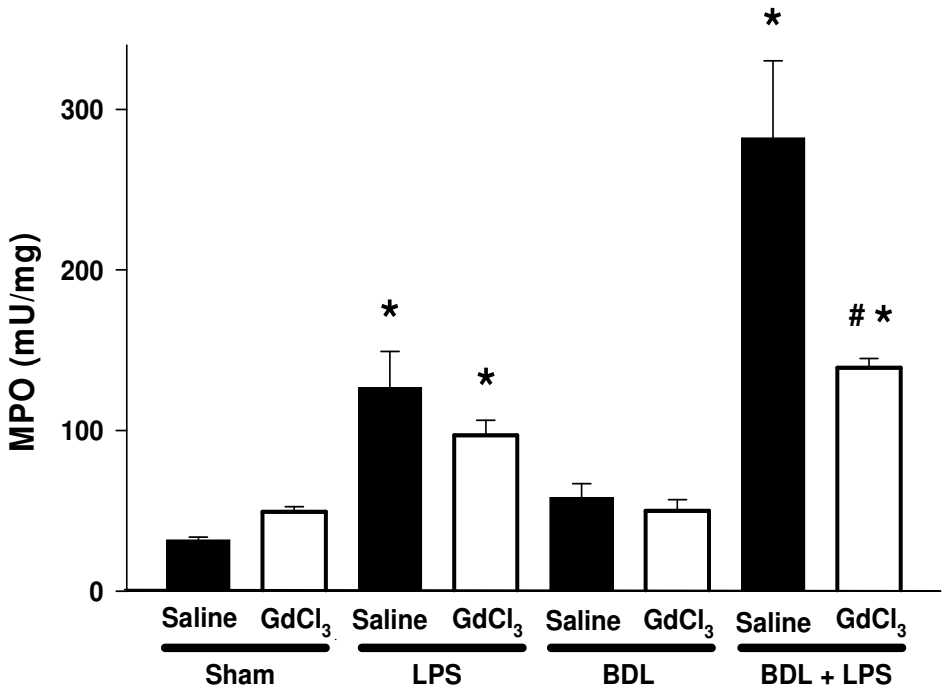

Figure 5. Changes in MPO activity in response to sham operation (Sham), endotoxemia induced with LPS, BDL or BDL + LPS (black bars), and the effects of $GdCl_3$ pretreatment (white bars). Data are presented as means ± SEM. * $P < 0.05$ *vs* Sham; # $P < 0.05$ *vs* Saline.

4.2.2. Changes in proinflammatory cytokine levels in the serum

The serum IL-6 and TNF-α levels were nearly undetectable in the sham-operated and BDL-challenged groups, but were elevated and exhibited similar tendencies of change after BDL + LPS (Figures 6A and B). Moreover, both the IL-6 and TNF-α levels were approximately 5 times higher after BDL + LPS than after LPS alone. $GdCl_3$ pretreatment inhibited only the TNF-α release in the animals challenged with LPS + BDL.

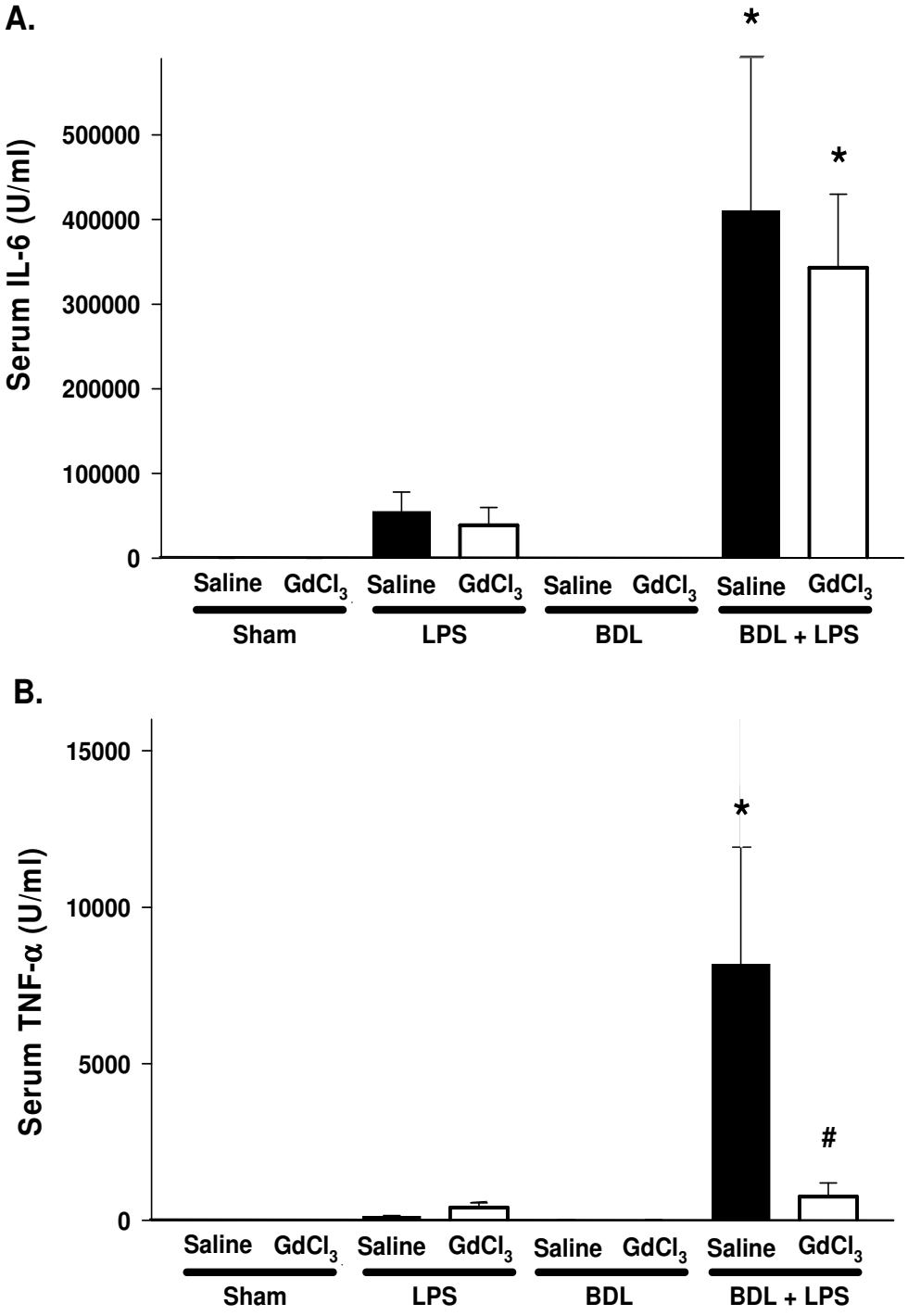

Figure 6. Effects of $GdCl_3$ pretreatment on the serum IL-6 (A) and TNF-α (B) levels in response to sham operation (Sham), endotoxemia induced with LPS, BDL or BDL + LPS (black bars), and the effects of $GdCl_3$ pretreatment (white bars). Data are presented as means ± SEM. * $P < 0.05$ *vs* Sham; # $P < 0.05$ *vs* Saline.

4.2.3. Changes in the induction of heme oxygenase and metallothionein

HO-1 appeared to be highly inducible by all of the stimuli employed (Figures 7A and B). Specifically, BDL caused an approximately 4-fold elevation, whereas LPS alone led to a nearly 10-fold elevation in this parameter. When LPS was combined with BDL, a similar extent of HO-1 induction was observed to that seen with LPS alone. In the sham-operated animals treated with $GdCl_3$, no changes in this parameter were detected, but the LPS or BDL + LPS-induced increases in HO-1 were significantly reduced following this intervention. HO-2 induction, however, led to a significant elevation (approximately 2-fold) only in the LPS-treated groups, where the alleviating effect of $GdCl_3$ was also evident (Figures 7A and C).

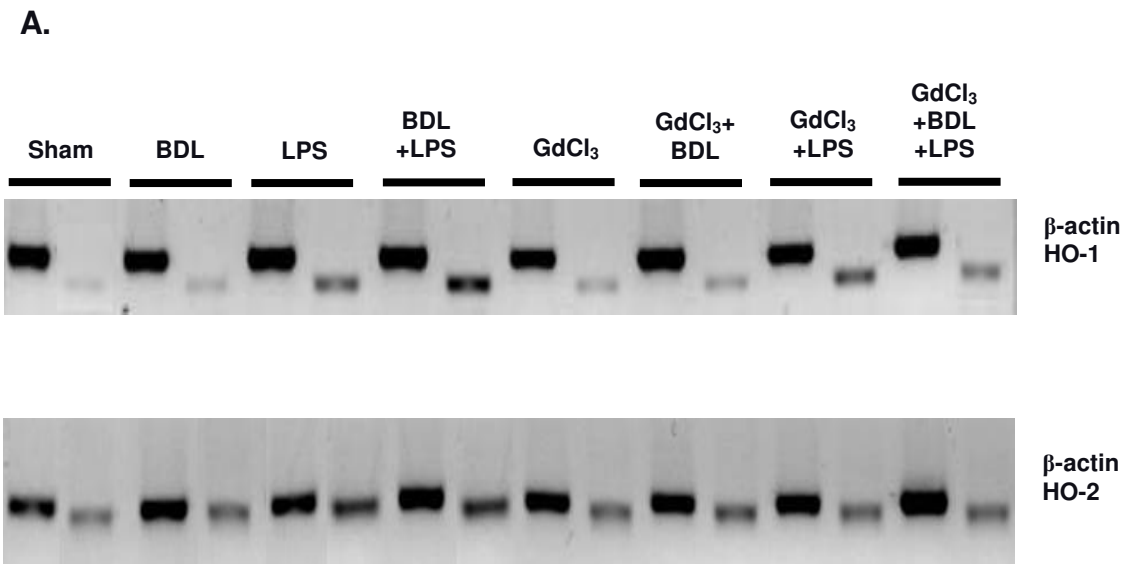

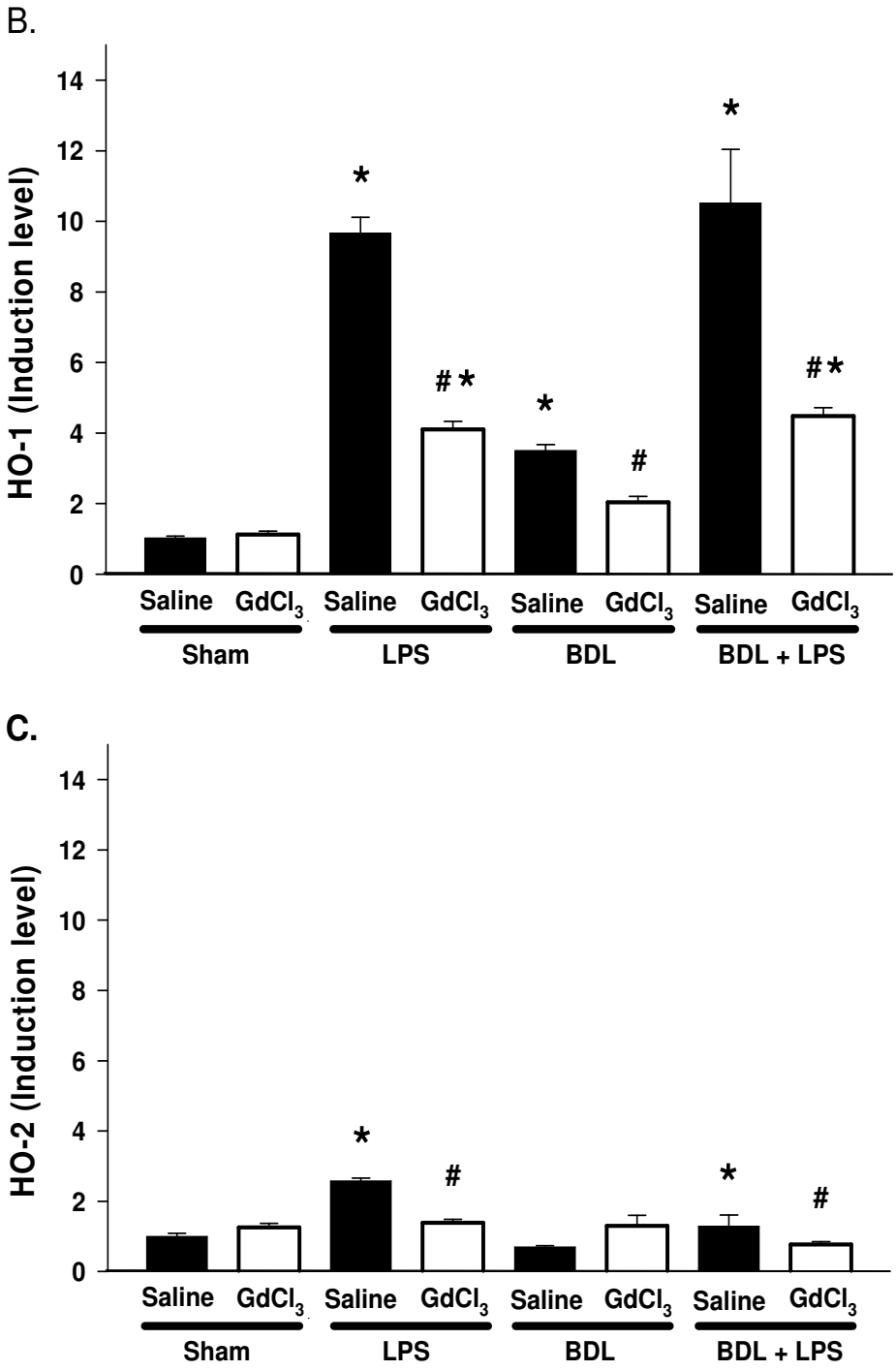

Figure 7. Representative RT-PCR amplification (A) demonstrating the hepatic expressions of HO-1 and HO-2 in response to sham operation (Sham), endotoxemia induced with LPS, BDL or BDL + LPS, and the effects of $GdCl_3$ pretreatment. The induction of HO-1 (B) and HO-2 (C) in response to the above challenges. Black bars denote the saline-treated animals, while the $GdCl_3$-pretreated animals are represented by white bars. Data are presented as means ± SEM. * $P < 0.05$ *vs* Sham; # $P < 0.05$ *vs* Saline.

No increases in the expression of the MT-1 gene were found in response to the different stimuli (Figures 8A and B), but an enhanced MT-2 gene expression (approximately 3.5-fold) could be demonstrated after LPS alone or when LPS was combined with BDL. No alterations in this parameter were observed in the vehicle-treated animals subjected to 3-day BDL. Significant and similar degrees of increase in MT-2 induction were found in all $GdCl_3$-treated groups, irrespective of the different challenges applied (Figures 8A and C).

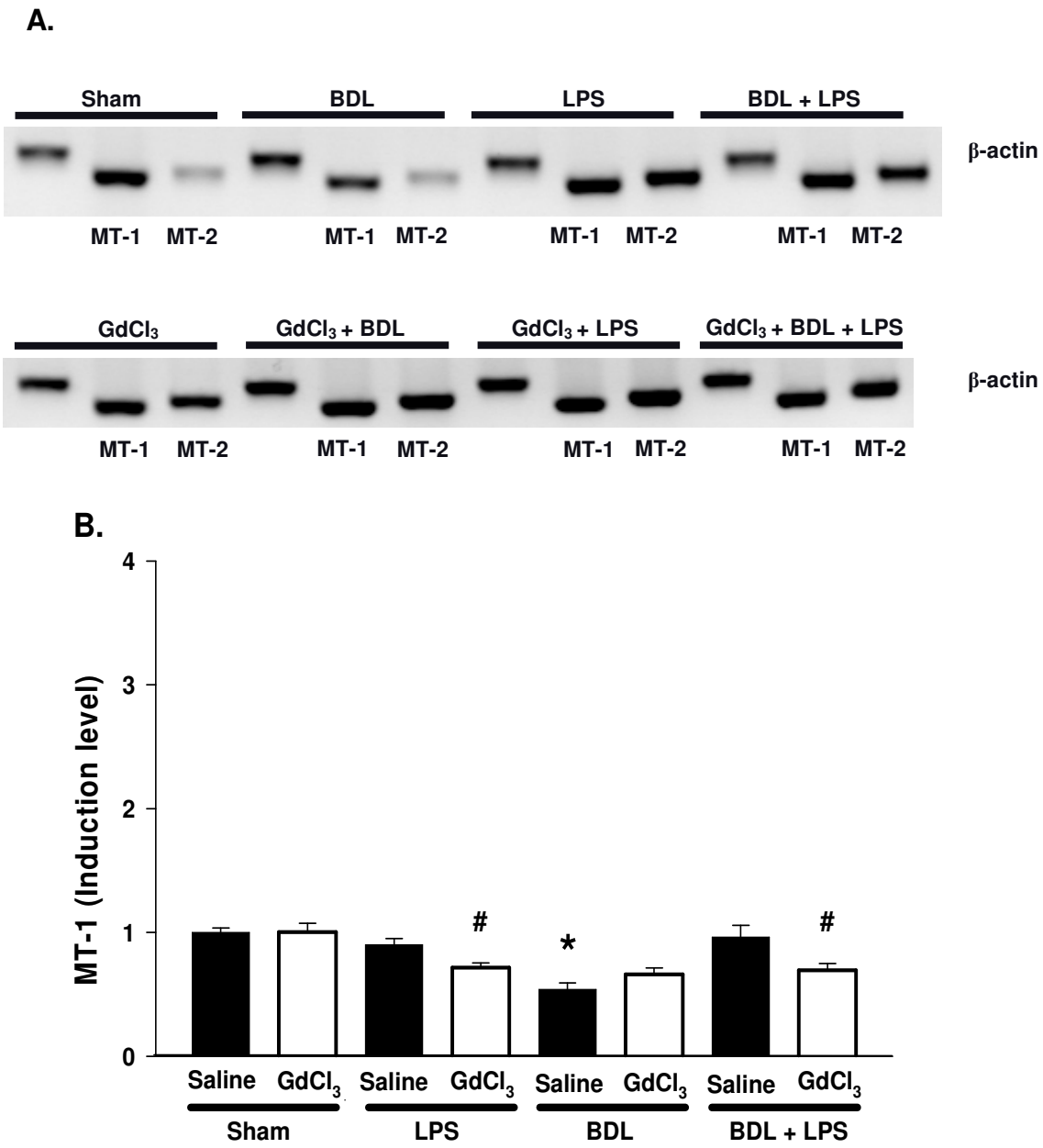

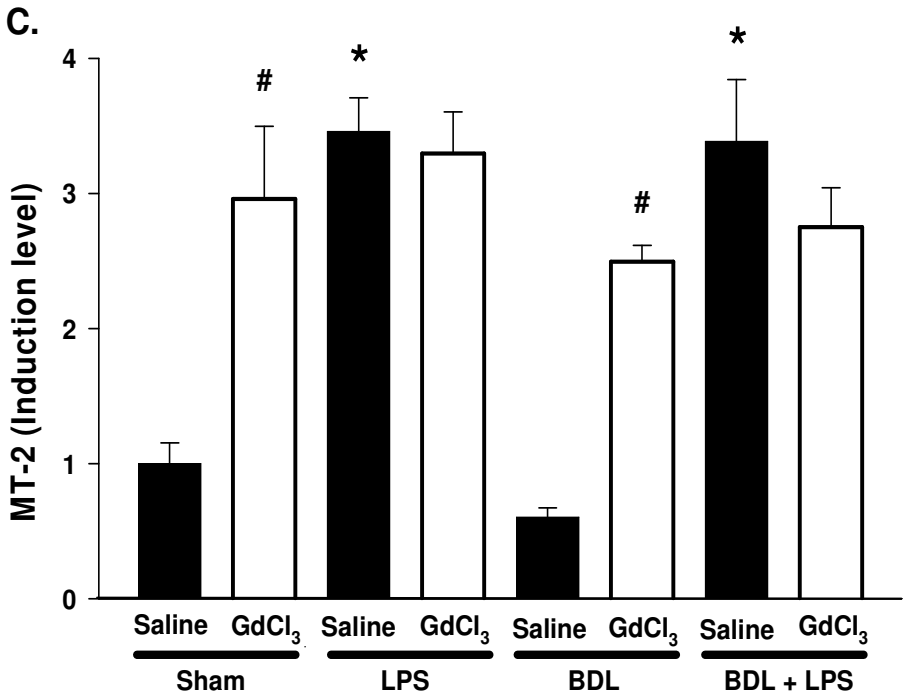

Figure 8. Representative RT-PCR amplification of MT-1 and 2, using total RNA as a template prepared from rat liver (A) and induction of MT-1 (B) and MT-2 (C) in response to sham operation (Sham), endotoxemia induced with LPS, BDL or BDL + LPS (black bars), and the effects of $GdCl_3$ pretreatment (white bars). Data are presented as means ± SEM. * $P < 0.05$ *vs* Sham; # $P < 0.05$ *vs* Saline.

4.2.4. Changes in the antioxidant defense system of the liver

As compared with the sham-operated animals, BDL and BDL + LPS caused severe (>50%) reductions in CAT activity, whereas LPS alone gave rise to an approximately 30% decrease in this parameter (Figure 9). $GdCl_3$ itself resulted in some reduction (by ~10%) in CAT activity. However, when $GdCl_3$ was applied in the presence of endotoxemia (or endotoxemia combined with BDL), it caused a partial restoration in CAT levels.

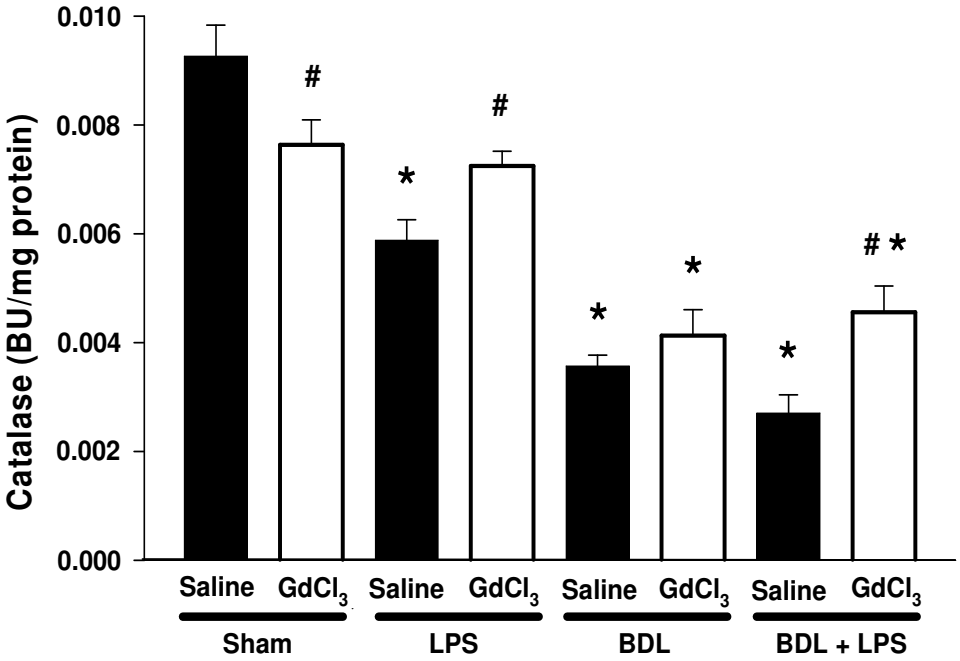

Figure 9. Changes in activity of CAT in response to sham operation (Sham), endotoxemia induced with LPS, BDL or BDL + LPS (black bars), and the effects of $GdCl_3$ pretreatment (white bars). Data are presented as means ± SEM. * $P < 0.05$ *vs* Sham; # $P < 0.05$ *vs* Saline.

An approximately 2-fold increase in Mn-SOD activity was found in all of the challenged groups (Figure 10A), but the Cu/Zn-SOD activity did not change significantly (Figure 10B); $GdCl_3$ did not affect these alterations.

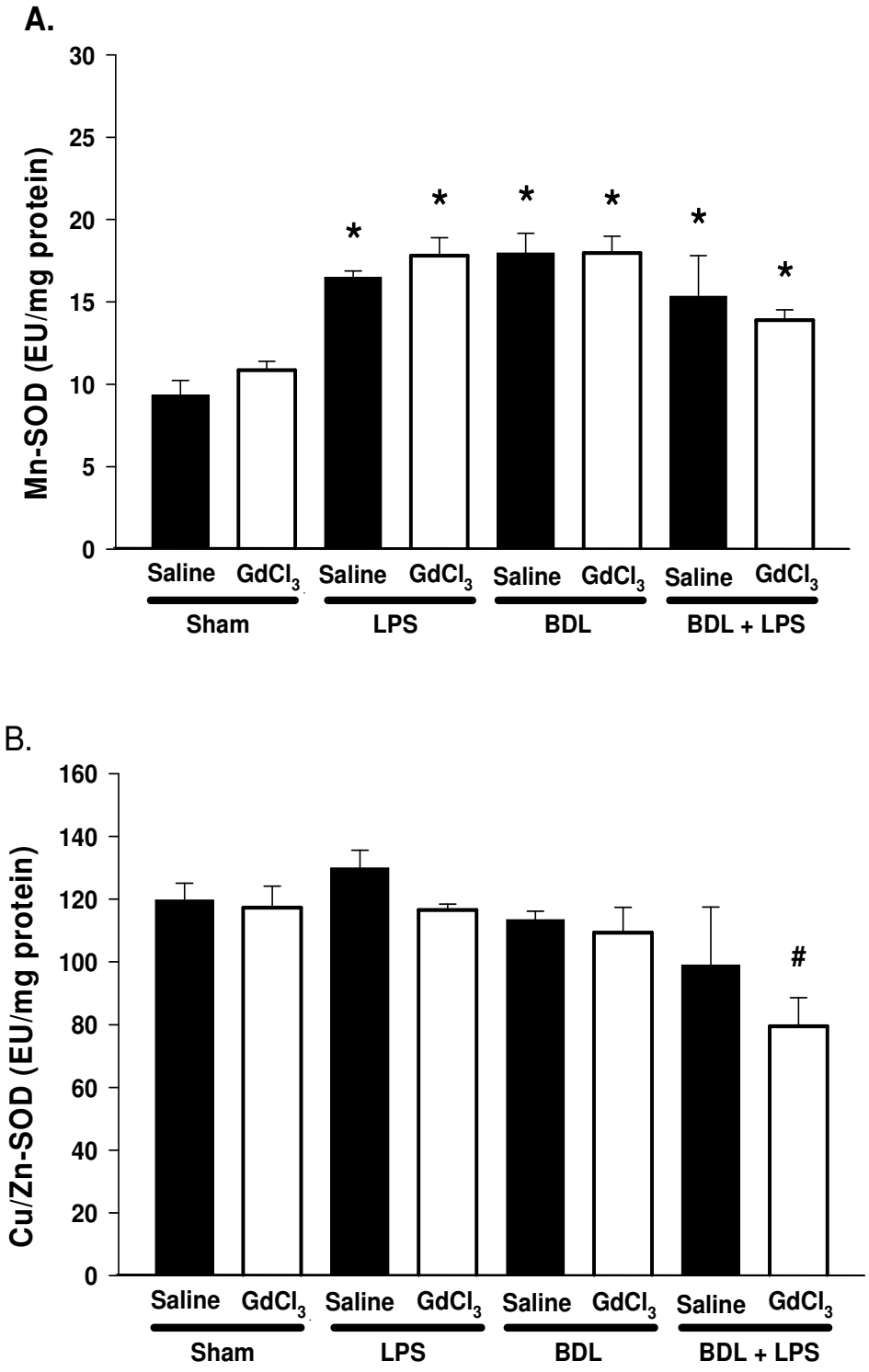

Figure 10. Changes in activity of Mn-SOD (A) and Cu/Zn-SOD (B) in response to sham operation (Sham), endotoxemia induced with LPS, BDL or BDL + LPS (black bars), and the effects of $GdCl_3$ pretreatment (white bars). Data are presented as means ± SEM. * $P < 0.05$ *vs* Sham; # $P < 0.05$ *vs* Saline.

4.2.5. Changes in hepatocellular damage

A moderately enhanced and comparable degree of DNA damage (approximately 4-fold) was observed in all challenged groups with or without KC blockade elicited by the heavy metal salt $GdCl_3$ (Figure 11), and a similar degree of DNA damage was also evidenced in response to this treatment alone. A lower level of DNA breakage was observed only in the animals challenged with BDL in the presence of $GdCl_3$ treatment.

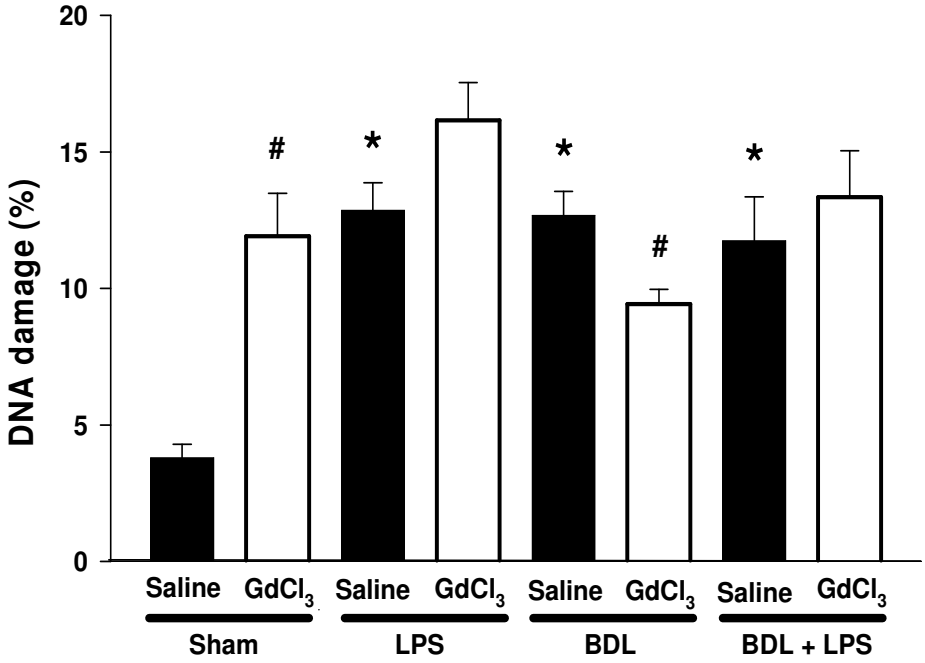

Figure 11. Extents of DNA damage in response to sham operation (Sham), endotoxemia induced with LPS, BDL or BDL + LPS (black bars), and the effects of $GdCl_3$ pretreatment (white bars). Data are presented as means ± SEM. * $P < 0.05$ *vs* Sham; # $P < 0.05$ *vs* Saline.

The MDA content in the liver was increased significantly (4-fold) only in the most severe condition, when endotoxemia was combined with BDL (Figure 12). $GdCl_3$ enhanced the LPO (2-3-fold) in all groups (including the sham-operated animals) and the degree of LPO again appeared to be independent of the type and severity of the challenge.

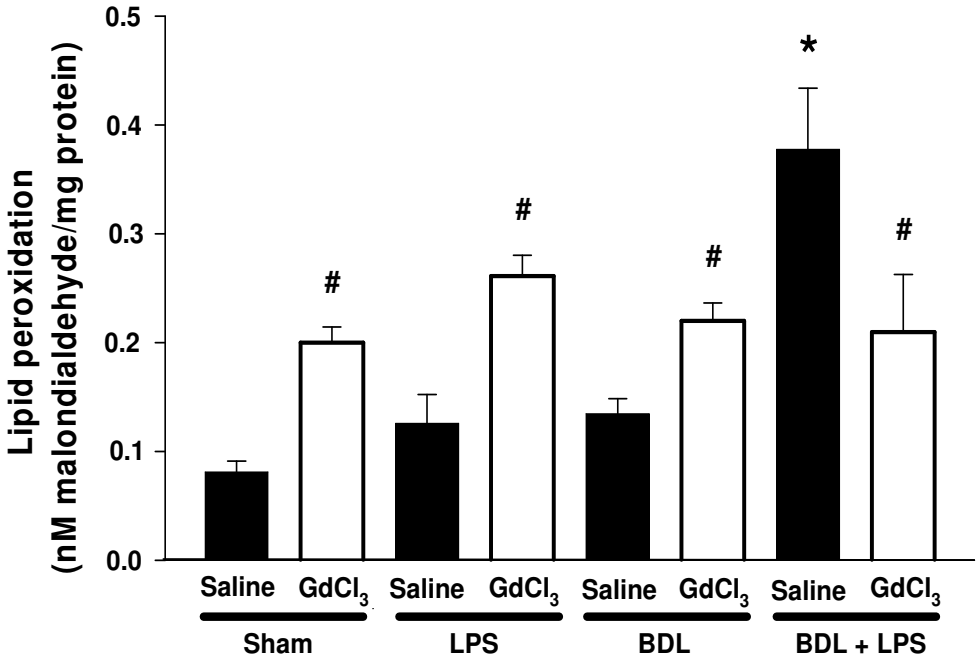

Figure 12. Extents of LPO in response to sham operation (Sham), endotoxemia induced with LPS, BDL or BDL + LPS (black bars), and the effects of $GdCl_3$ pretreatment (white bars). Data are presented as means ± SEM. * $P < 0.05$ *vs* Sham; # $P < 0.05$ *vs* Saline.

4.3. Histological damage in the liver

Histological evaluation was performed in the portal, periportal and intralobular regions of the liver (Table 1, Figure 13). The sham operation or LPS treatment did not induce considerable structural alterations in any of the regions examined. The present grading system indicated that BDL and BDL + LPS caused the most marked damage in the portal region, but structural damage was also evident in the periportal and intralobular regions. Interestingly, the above histological alterations were similar in the BDL and BDL + LPS groups. These changes were not influenced by the KC blockade in the portal and intralobular regions, but were completely abolished in the periportal area. Data are expressed as means ± SEM ∗ $P < 0.05$ *vs* Sham + vehicle; # $P < 0.05$ *vs* corresponding vehicle-treated group.

Groups	Periportal score	Portal score	Intralobular score
Sham + vehicle	0.00 ± 0.00	1.00±0.32	0.00 ± 0.00
Sham + $GdCl_3$	0.00 ± 0.00	0.60 ± 0.30	0.00 ± 0.00
BDL + vehicle	0.60 ± 0.40	3.20±0.20 *	0.53 ± 0.08
BDL + $GdCl_3$	0.00 ± 0.00	2.80±0.37 *	0.26± 0.07
LPS + vehicle	0.00 ± 0.00	0.80±0.20	0.00 ± 0.00
LPS + $GdCl_3$	0.00 ± 0.00	0.40±0.25	0.20 ± 0.13
BDL + LPS	2.00 ± 0.55 *	3.40±0.25 *	0.26 ± 0.07
BDL + LPS + $GdCl_3$	0.00 ± 0.00 #	4.00±0.32 *	0.86 ± 0.17

Table 1. Effects of $GdCl_3$ pretreatment on the hepatic histological injury in portal, periportal and intralobular regions in response to sham operation (Sham), endotoxemia (LPS), and BDL + LPS. Data are presented as means ± SEM. * $P < 0.05$ *vs* Sham; # $P < 0.05$ *vs* Saline.

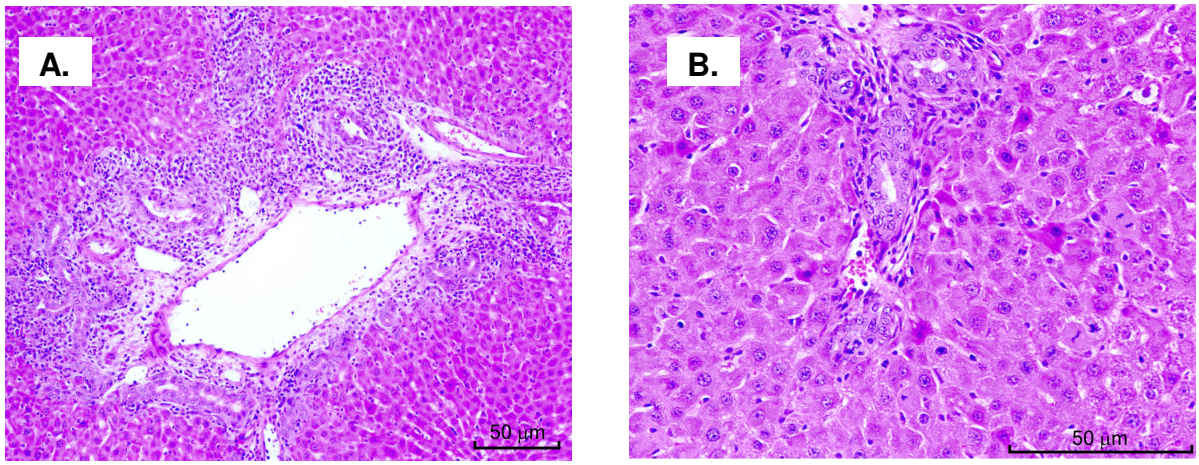

Figure 13. Light microscopic images of the liver tissue. Severe hepatic damage with piecemeal necrosis in the BDL + LPS group (A) (H&E; original magnification 224x) and ameliorated hepatic inflammatory signs in the BDL + LPS group pretreated with $GdCl_3$ (B) (H&E; original magnification 400x).

5. DISCUSSION

The survival rate of critically ill patients with obstructive jaundice has not improved in recent decades and septic complications are still the leading causes of mortality in this condition (Greig JD, 1988; Diamond T, 1990). In line with this, the experimental data suggest that biliary obstruction enhances the inflammatory and microvascular responses of the liver to endotoxemia (Ito Y, 2000; Lázár G Jr, 2002). Our results provide further support of these findings since the hepatic microcirculatory dysfunction was significantly exaggerated when obstructive jaundice was followed by an LPS challenge. The results also show that the hepatic KCs play a pivotal role in this process.

We used a rodent model to mimic the inflammatory complications of cholestasis at the microcirculatory level. The methods applied in this study enabled us to examine the inter-relationship between various microcirculatory parameters and to compare these events with structural alterations in the liver under different circumstances. First, we found that obstructive jaundice and endotoxemia caused characteristically different microcirculatory responses in the liver. Specifically, LPS induced considerable leukocyte activation, but, this was not accompanied by a severe hepatic perfusion failure (see also Bauer M, 1994;Vollmar B, 1996). In contrast, BDL resulted in a significantly reduced capillary perfusion, and the leukocyte accumulation was only moderate. A strong causal relationship has been suggested between leukocyte sticking and decreased capillary perfusion (Zhang JX, 1994). It is difficult to compare different models and different time frames, but our observations do not support this generalized statement. Nonetheless, the observation time with the presented BDL model is prolonged and it can not be excluded that earlier microvascular perfusion alterations are followed by PMN-induced hepatic inflammation in later phases. Indeed, an increased adhesion molecule expression and PMN adherence were observed only in the later stages of obstructive jaundice (Koeppel TA, 1997; Ito Y, 2003). Nonetheless, our data suggest characteristically different microcirculatory responses in the time frame of the present studies.

In our previous study with 24 h of endotoxemia and 6 days of BDL, we demonstrated that histological liver injury is preceded by functional changes (Lázár G Jr, 2002). Our present data permit an evaluation of the impact of the different microcirculatory changes on the final outcome of liver injury hallmarked by histological damage. The most severe structural

alterations in all liver parts were caused by BDL, which was accompanied primarily by a hepatic perfusion failure, and not by inflammatory reactions (*i.e.* neutrophil activation and accumulation, and TNF-α release). Moreover, the microcirculatory consequences of a 3-day BDL were exacerbated by 1-h endotoxemia (a perfusion deficit, the tissue accumulation of leukocytes and the release of proinflammatory cytokines) (see also Ito Y, 2000). Interestingly, these changes were not manifested in considerable alterations at the histological level in the short run. Even so, these observations suggest the impact of impaired tissue perfusion over the inflammatory reactions on the histological injury formation in the examined time frame. As cumulative injury should be presumed with all forms of BDL, the appraisal of these alterations requires careful consideration.

All the models used in these studies were accompanied by a considerably increased KC activation, which could be partially blocked with $GdCl_3$. The blockade elicited by this administration, however, beneficially influenced most of the examined parameters, such as the leukocyte adhesion and migration, the TNF-α release, the HO and MT activities and the structural damage in the periportal region, even in the cases with the most severe combined challenges.

It has been demonstrated that the KCs are primary sources of circulating TNF-α and IL-6 in response to LPS (Hoffmann R, 1994). Additionally, both experimental and clinical observations indicate that the KCs are involved in the increased cytokine secretion in obstructive jaundice (Bemelmans MH, 1992; Puntis MC, 1996; O'Neil S, 1997). In accordance with these findings, we found excessive proinflammatory cytokine release after LPS administration in BDL animals, accompanied by an increased KC activity. Moreover, our present data suggest that the higher susceptibility to endotoxemia during obstructive jaundice involves KC activation. This suggests a sensitizing triggering mechanism which can lead to the exaggeration of inflammation after repeated stimuli or if the injury is prolonged. Some authors emphasize the direct effect of a biliary obstruction on the hepatocytes and KCs (Diamond T, 1991). Others have underlined the importance of the elevated LPS-binding protein in the pathomechanism (Kimmings AN, 2000; Albillos A, 2004). This latter hypothesis is supported by the studies of Minter *et al.* (Minter RM, 2005), showing that KCs isolated from experimental animals with BDL are exquisitely sensitive to LPS-binding protein, but not to LPS.

A regulatory role in the maintenance of the hepatic microcirculation has been attributed to KCs by some authors (Ruttinger D, 1996; Keller SA, 2005). In general, the liver microcirculation is determined by a balance between vasoconstrictor and vasodilator forces (Pannen BH, 1996). The plasma levels of endothelin-1 (ET-1) increase in endotoxemia (Pannen BH, 1996), sepsis and clinical and experimental biliary obstruction. It has been shown that KC depletion improves the septic liver microcirculation by reducing the hypercontractile response to ET-1 (Keller SA, 2005). Moreover, it has been demonstrated that $GdCl_3$ pretreatment decreases the hepatic ET-1 secretion, leading to improved hepatic micro- and macroperfusion after warm ischemia (Frankenberg MV, 2005). It has also been that ET-1 triggers the release of other vasoconstrictive mediators such as thromboxane-2 (TXA_2) in the endotoxemic liver, which mediate the hyperresponsiveness of the portal circulation to ETs (Xu H, 2005). The study by Xu et al. showed that KCs are the major source of the increased release of TXA_2 into the portal system in response to ET-1 during acute endotoxemia (Xu H, 2005). Furthermore, BDL in combination with LPS additively activated the KCs, with an upregulation of the key enzymes in the TXA_2 biosynthesis in response to ET-1, which eventually contributes to the development of a hepatic microcirculatory dysfunction (Miller AM, 2007). Taken together, these data clearly confirm the central role of KCs in the regulation of the hepatic microcirculation in this scenario.

The biochemical parameters also show characteristic changes. The sensitivity of the liver to inflammatory conditions is illustrated by the fact that the MT and HO gene expressions are more inducible in the liver than in other organs (De SK, 1990; Hur T, 1999). As the production of these proteins is mostly regulated at the transcriptional level, the expressions of their genes and not their protein levels were subjected to examination in our present models. Such regulation of these genes was apparent in these observations: only the induction of the HO-1 and MT-2 isoforms changed considerably, with the induction level dependent on the stimulus applied. As concerns HO-1, its increased expression is regarded as a sign of the activation of an endogenous protective reaction in response to oxidative stress (Tüzüner E, 2004). In our study, a moderately increased induction of hepatic HO-1 was observed even as late as 3 days after the BDL. It is noteworthy, however, that the level of HO-1 induction was higher in the acute phase of endotoxemia than in the later phase of obstructive jaundice. The HO-2 changes demonstrated a similar tendency, with markedly

lower induction levels. It is reasonable to assume that endotoxemia alone results in a close to maximal induction of the HO gene, since these changes could not be further enhanced when the BDL and LPS challenges were combined. Furthermore, our measurements were performed at a stage of endotoxemia when the TNF-α levels had attained their maximal values; the elevations in level of this proinflammatory cytokine are effectively prevented by this method of KC blockade (Rizzardini M, 1998). Since TNF-α is a potential enhancer of HO-1 mRNA expression (Oguro T, 2002), the lower extent of HO-1 induction may also result from the reducing effect of KC blockade on the TNF-α expression. Hence, the lower induction of HO-1 in the presence of $GdCl_3$ is most probably a consequence of a potentially reduced hepatic injury, as a direct inhibitory effect of $GdCl_3$ on HO-1 gene expression has not been described.

Another manifestation of the stress-induced hepatic response is induction of the MT gene, which has been described in the early phase of endotoxemia (Choudhuri S, 1993; Giralt M, 1993) and in biliary obstruction (Brambila E, 2000). To the best of our knowledge, the isoform-specific changes in hepatic MT expression observed under the above circumstances in the present study are described for the first time here. Similarly to the HO-1 changes, the induction of MT-2 (but not MT-1) peaked after acute endotoxemia and was not enhanced when LPS was combined with BDL. The dependence of the expression of MT-2 on the time course of BDL can not be ruled out (and could not be assessed in the present study); nonetheless, the induction of this gene was not found to be elevated 3 days after BDL. Further studies are needed to elucidate why additive effects of these challenges are not observed for the above gene (HO and MT) expressions, even though LPS has been shown to worsen the consequences of BDL both experimentally (Harry D, 1999) and in clinical practice (Greig JD, 1988).

In response to $GdCl_3$ treatment, similar isoform-specific elevations in MT-2 induction have been observed, but these were virtually independent of the noxious stimulus (Andrés D, 2003). It is conceivable that the mechanisms of MT induction in endotoxemia and after $GdCl_3$ are different. It is likely that the MT mRNA expression elevation is related to the injury caused by free radicals in the case of endotoxemia, whereas MT induction is a direct consequence of the metal ion overload caused by the heavy metal ion Gd^{3+}. The MT proteins are believed to be protective in nature, representing an intrinsic protective mechanism in

endotoxemia (Takano H, 2004) as well as against heavy metal-induced oxidative damage (Chubatsu LS, 1993) and against cadmium toxicity (Michalska, AE, 1993; Masters BA, 1994; Liu J, 1996). The exact consequences of MT-2 induction are also a potential subject of further examinations, targeting the questions of whether (1) only the MT-2 expression remains elevated, (2) binding between $GdCl_3$ and MTs still exists 24 h after the treatment, and (3) if so, how it influences the free radical-scavenging capacity of MT.

In our experiments, all of the noxious stimuli led to a similar, albeit moderate degree of hepatic DNA single-strand break formation. An increased level of LPO was observed only when BDL and LPS were combined. $GdCl_3$ alone caused elevations in both parameters (particularly in LPO) (Ruttinger D, 1997). The hepatotoxic effects of $GdCl_3$ have been reported elsewhere (Paxian M, 2001). Our models demonstrated that the free radical-derived hepatotoxicity overwhelms the endogenous hepatic protective antioxidant mechanisms. This is manifested in the characteristic changes in the CAT and Mn-SOD activities, which may reflect the cumulative effect of free radical toxicity, referring also to the time frame of the challenges. With respect to the CAT activity, BDL and BDL combined with LPS comprise a stronger signal than acute endotoxemia alone. Our results support observations that endotoxemia leads to a decrease in hepatic CAT activity (Llesuy S, 1994; Spolarics Z, 1996; Zhong Z, 2002) and we additionally observed a simultaneous increase in Mn-SOD activity. Most BDL studies have yielded similar results concerning CAT activity, but usually the total SOD activities are determined (Singh S, 1992; Orellana M, 2000; El-Sayed, IH, 2003; Padillo FJ, 2004). In our study with BDL, the mitochondrial Mn-SOD activity was found to increase, with a simultaneous decrease in the cytosolic Cu/Zn-SOD level. We also determined the changes in other components of the superoxide-targeting antioxidant machinery, the levels of reduced glutathione and glutathione peroxidase, but these varied only insignificantly in response to any of the challenges applied (data not shown). Despite its mentioned toxic effects, a moderate protective effect of $GdCl_3$ was revealed in its partial restoration of the CAT levels in our two models involving endotoxemia.

In view of our present data, the role of $GdCl_3$ is rather controversial. $GdCl_3$ induces some degree of subcellular damage (reflected by the LPO), but despite the hepatotoxic effect attributed to this compound (Paxian M, 2001), it has been demonstrated to alleviate the injury caused by agents such as cadmium chloride (Harstad EB, 2002) or retinol (Sauer JM, 2005).

The toxicity of Gd^{3+} depends on the dose and the chemical form (hydroxylated/protein complex form) (Ding H, 2003). Our present data suggest that it would also be important to establish whether any effect of $GdCl_3$ on the antioxidant CAT levels is related to its own toxicity or to its action on the basic challenge models themselves. We believe that the protective effects of $GdCl_3$ (earlier shown to reduce microcirculatory failure, microcirculatory inflammation, structural damage and inflammatory cytokine release (Lázár G Jr, 2002)) reflect the obvious predominance of the beneficial effects of this compound. The unfavorable subcellular effects, however, warrant caution.

Our present observations should finally be discussed in view of the final end-points of hepatic injury. We believe that the final outcome of the challenges applied corresponds strongly with the functional and structural impairment of the liver. The clinical observations supported the previous demonstration that the histological structural damage and functional (*e.g.* microcirculatory) impairment of the liver caused by biliary obstruction are aggravated by endotoxemia. Acute endotoxemia causes a lesser degree of injury and KC blockade with $GdCl_3$ beneficially influences most of the consequences of the above challenges (Lázár G Jr, 2002). In the present study, we also targeted the endogenous antioxidant activities (SOD and CAT), together with an isoform-specific assessment of other proteins which also possess free radical-scavenging properties (HO and MT). The results demonstrate that 2 h of endotoxemia comprises a stronger signal for the induction of a stress response (*e.g.* HO-1 and MT-2) than that of a 3-day biliary obstruction (despite the similar degree of hepatic DNA and membrane damage). The combination of these challenges results in more severe alterations only in LPO. We have also established that, although $GdCl_3$ induces some degree of LPO and DNA damage independently of the various challenges, its alleviating effects are also evident, as the stress-induced induction of HO-1 is reduced and the CAT levels are partially restored in the presence of this intervention. These signs of ameliorated stress-induced hepatic reactions provided by $GdCl_3$ may contribute to its beneficial hepatic protective effects.

6. SUMMARY OF NEW FINDINGS

1. The inflammatory complications of obstructive jaundice are greatly deteriorated if a second hit of endotoxemia is elicited. These inflammatory reactions are manifested in an impairment of the microcirculatory perfusion, the activation and accumulation of leukocytes and enhanced proinflammatory cytokine release.

2. A causal relationship between the hepatic microcirculatory and histological changes after biliary obstruction can be assumed, whereas inflammatory reactions (leukocyte activation) may exert only a relatively minor influence in these factors.

3. Acute endotoxemia comprises a stronger signal for the induction of a stress response (*e.g.* HO-1 and MT-2) than that of a 3-day biliary obstruction (despite the similar degree of hepatic DNA and membrane damage). The combination of these challenges results in more severe alterations only in LPO.

4. KC blockade with $GdCl_3$ reduces the detrimental microcirculatory consequences of endotoxemia, and beneficially influences the inflammatory reactions when obstructive jaundice is combined with an LPS challenge. The $GdCl_3$ treatment ameliorated the KC and leukocyte activations, the TNF-α release and the tissue accumulation of the PMNs.

5. $GdCl_3$ alone induces some degree of LPO and DNA damage independently of the various challenges, but its alleviating effects are also evident, as the stress-induced induction of HO-1 is reduced and the CAT levels are partially restored in the presence of this intervention.

6. KC blockade ameliorates inflammatory complications of obstructive jaundice by beneficially influencing the microvascular inflammatory reactions with simultaneous positive effects on hepatic biochemical processes and structural injury.

7. ACKNOWLEDGEMENTS

I am deeply grateful to my supervisor, Professor György Lázár Jr., Head of the Department of Surgery, University of Szeged, for his patience, his encouraging attitude and his valuable advice, and for providing me with the opportunity to perform my studies.

My special thanks to Professor Mihály Boros and Professor György Lázár Sr. for their valuable scientific guidance and help.

I am indebted are due to Andrea Szabó, who helped me learn the basic experimental skills and granted me indispensable assistance in preparing the manuscripts.

I thank Edit Hermesz for her contribution in the molecular biological evaluations.

I would like to express my thanks to all my co-workers with whom I performed the experiments: Ernő Duda, Katalin Éder, Ágnes Ferencz, József Kaszaki, Attila Paszt, László Tiszlavicz and Renáta Varga.

Special thanks are also due to Anna Kancsár from the Institute of Pathophysiology and all the technical staff of the Institute of Surgical Research.

Finally, I would like to give my special thanks to my family, and especially to my mother, Magdolna Ábrahám, my father, Tamás Ábrahám, and my wife, Enikő Csonka, whose patient love has enabled me to complete this work.

8. REFERENCES

Abe S, Matsumi M, Tsukioki M, Mizukawa S, Takahashi T, Iijima Y, Itano Y, Kosaka F. Metallothionein and zinc metabolism in endotoxin shock rats. *Experientia Suppl* 52:587-94, 1987.

Aggarwal BB, Kohr WJ, Hass PE. Human tumor necrosis factor production, purification and characterization. *J Biol Chem* 260:2345-2354, 1985.

Albillos A, de-la-Hera A, Alvarez-Mon M. Serum lipopolysaccharide-binding protein prediction of severe bacterial infection in cirrhotic patients with ascites. *Lancet* 363:1608-1610, 2004.

Andrés D, Sánchez-Reus I, Bautista M, Cascales M. Depletio of Kupffer cell function by gadolinium chloride attenuates thioacetamide-induced hepatotoxicity. Expression of metallothionein and HSP70. *Biochem Pharmacol* 66:917-26, 2003.

Armstrong CP, Dixon JM, Taylor TV, Davies GC. Surgical experience of deeply jaundiced patients with bile duct obstruction. *Br J Surg* 71:234-8, 1984.

Ball SK, Grogan JB, Collier BJ, Scott-Conner CE. Bacterial phagocytosis in obstructive jaundice. A microbiologic and electron microscopic analysis. *Am Surg* 57:67-72, 1991.

Barriault C, Audet M, Yousef IM, Tuchweber B. Effect of agents which modify reticuloendothelial system function on acute phalloidin-induced lethality and hepatotoxicity in mice. *Toxicol Appl Pharmacol* 31:206-215, 1995.

Bauer I, Wanner GA, Rensing H, Alte C, Miescher EA, Wolf B, Pannen BH, Clemens MG, Bauer M. Expression pattern of heme oxygenase isoenzymes 1 and 2 in normal and stress-exposed rat liver. *Hepatology* 27:829-38, 1998.

Bauer M, Marzi I, Thuma B, Bach F, Buhren V, Larsen R. Dose-related pattern of sinusoidal leukocyte adhesion in sublobular regions of the liver after systemic endotoxin challenge in the rat. *Shock* 1:135-140, 1994.

Beauchamp C, Fridovich I. Superoxide dismutase. Improved assays and an assay applicable to acrylamide gels. *Anal Biochem* 44:276-287, 1971.

Beers RF Jr, Sizer IW. A spectrophotometric method for measuring the breakdown of hydrogen peroxide by catalase. *J Biol Chem* 195:133-140, 1952.

Bemelmans MH, Gouma DJ, Greve JW, Buurman WA. Cytokines tumor necrosis factor and interleukin-6 in experimental biliary obstruction in mice. *Hepatology* 15:1132-1136, 1992.

Blamey SL, Fearon KC, Gilmour WH, Osborne DH, Carter DC. Prediction of risk in biliary surgery. *Br J Surg* 70:535-8, 1983.

Bonfanti R, Furie BC, Furie B, Wagner DD. PADGEM (GMP140) is a component of Weibel-Palade bodies of human endothelial cells. *Blood* 73:1109–12, 1989.

Brambila E, Munoz-Sanchez JL, Waalkes MP, Albores A. Effect of surgically induced cholestasis on the levels of hepatic zinc and metallothionein in rat liver. *Biol Trace Elem Res* 78: 255-264, 2000.

Busam KJ, Bauer TM, Bauer J, Gerok W, Decker K. Interleukin-6 release by rat liver macrophages. *J Hepatol* 11:367-73, 1990.

Camhi SL, Lee P, Choi AM. The oxidative stress response. *New Horiz* 3:170-82, 1995.

Carrico CJ. The elusive pathophysiology of the multiple organ failure syndrome. *Ann Surg* 218:109-10, 1993.

Chosay JG, Essani NA, Dunn CJ, Jaeschke H. Neutrophil margination and extravasation in sinusoids and venules of liver during endotoxin-induced injury. *Am J Physiol* 272:G1195-200, 1997.

Choudhuri S, McKim JM Jr, Klaassen CD. Differential expression of the metallothionein gene in liver and brain of mice and rats. *Toxicol Appl Pharmacol* 119:1-10, 1993.

Chubatsu LS, Meneghini R. Metallothionein protects DNA from oxidative damage. *Biochem J* 291:193-8, 1993.

Crofton RW, Diesselhoff-den Dulk MM, van Furth R. The origin, kinetics, and characteristics of the Kupffer cells in the normal steady state. *J Exp Med* 148:1-17, 1978.

De SK, McMaster MT, Andrews GK. Endotoxin induction of murine metallothionein gene expression. *J Biol Chem* 265:15267-74, 1990.

Diamond T, Dolan S, Thompson RL, Rowlands BJ. Development and reversal of endotoxemia and endotoxin-related death in obstructive jaundice. *Surgery* 108:370-374, 1990.

Diamond T, Rowlands BJ. Endotoxaemia in obstructive jaundice. *HPB Surg* 4:81-94, 1991.

Ding H, Peng R, Reed E, Li QQ. Effects of Kupffer cell inhibition on liver function and hepatocellular activity in mice. *Int J Mol Med* 12:549-57, 2003.

Ding JW, Andersson R, Norgren L, Stenram U, Bengmark S. The influence of biliary obstruction and sepsis on reticuloendothelial function in rats. *Eur J Surg* 158:157-164, 1992.

El-Sayed IH, El-Kady IM, Badra GA. The effect of endoscopic retrograde cholangiopancreatography on the serum IL-18 and erythrocytes antioxidative capacity in biliary obstructive jaundice. *Clin Chim Acta* 336:123-8, 2003.

Eppihimer MJ, Wolitzky B, Anderson DC, Labow MA, Granger DN. Heterogeneity of expression of E- and P-selectins in vivo. *Circ Res* 79:560–9, 1996.

Frankenberg MV, Weimann J, Fritz S, Fiedler J, Mehrabi A, Buchler MW, Kraus TW. Gadolinium chloride-induced improvement of postischemic hepatic perfusion after warm ischemia is associated with reduced hepatic endothelin secretion. *Transpl Int* 18:429-436, 2005.

Fridovich I. Superoxide radical and superoxide dismutases. *Annu Rev Biochem* 64:97-112, 1995.

Froh M, Conzelmann L, Walbrun P, Netter S, Wiest R, Wheeler MD, Uesugi T, Scholmerich J, Thurman RG. Heme oxygenase-1 overexpression increases liver injury after bile duct ligation in rats. *World J Gastroenterol* 13:3478-86, 2007.

Gehring S, Dickson EM, San Martin ME, van Rooijen N, Papa EF, Harty MW, Tracy TF Jr, Gregory SH. Kupffer cells abrogate cholestatic liver injury in mice. *Gastroenterology* 130:810-822, 2006.

Gemsa D, Woo CH, Fudenberg HH, Schmid R. Stimulation of heme oxygenase in macrophages and liver by endotoxin. *J Clin Invest* 53:647-51, 1974.

Giakoustidis DE, Iliadis S, Tsantilas D, Papageorgiou G, Kontos N, Kostopoulou E, Botsoglou NA, Gerasimidis T, Dimitriadou A. Blockade of Kupffer cells by gadolinium chloride reduces lipid peroxidation and protects liver from ischemia/reperfusion injury. *Hepatogastroenterology* 50:1587-92, 2003.

Giralt M, Gasull T, Blánquez A, Hidalgo J. Effect of endotoxin on rat serum, lung and liver lipid peroxidation and on tissue metallothionein levels. *Rev Esp Fisiol* 49:73-8, 1993.

Greig JD, Krukowski ZH, Matheson NA. Surgical morbidity and mortality in one hundred and twenty-nine patients with obstructive jaundice. *Br J Surg* 75:216-219, 1988.

Gutteridge JM. Lipid peroxidation and antioxidants as biomarkers of tissue damage. *Clin Chem* 41:1819-28, 1995.

Harstad EB, Klaassen CD. Gadolinium chloride pretreatment prevents cadmium chloride-induced liver damage in both wild-type and MT-null mice. *Toxicol Appl Pharmacol* 180:178-85, 2002.

Harry D, Anand R, Holt S, Davies S, Marley R, Fernando B, Goodier D, Moore K. Increased sensitivity to endotoxemia in the bile duct-ligated cirrhotic rat. *Hepatology* 30:1198-1205, 1999.

Hoffmann R, Grewe M, Estler HC, Schulze-Specking A, Decker K. Regulation of tumor necrosis factor-alpha-mRNA synthesis and distribution of tumor necrosis factor-alpha-mRNA synthesizing cells in rat liver during experimental endotoxemia. *J Hepatology* 20:122-128, 1994.

Hur T, Squibb K, Cosma G, Horowitz S, Piedboeuf B, Bowser D, Gordon T. Induction of metallothionein and heme oxygenase in rats after inhalation of endotoxin. *J Toxicol Environ Health A* 56:183-203, 1999.

Husztik E, Lázár G, Parducz A. Electron microscopic study of Kupffer-cell phagocytosis blockade induced by gadolinium chloride. *Br J Exp Pathol* 61:624-630, 1980.

Ito Y, Bethea NW, Baker GL, McCuskey MK, Urbaschek R, McCuskey RS. Hepatic microcirculatory dysfunction during cholestatic liver injury in rats. *Microcirculation* 10:421-432, 2003.

Ito Y, Machen NW, Urbaschek R, McCuskey RS. Biliary obstruction exacerbates the hepatic microvascular inflammatory response to endotoxin. *Shock* 14:599-604, 2000.

Jacob AI, Goldberg PK, Bloom N, Degenshein GA, Kozinn PJ. Endotoxin and bacteria in portal blood. *Gastroenterology* 72:1268-70, 1977.

Jung JY, Lee SM. The roles of Kupffer cells in hepatic dysfunction induced by ischemia/reperfusion in rats. *Arch Pharm Res* 28:1386-91, 2005.

Katz S, Grosfeld JL, Gross K, Plager DA, Ross D, Rosenthal RS, Hull M, Weber TR. Impaired bacterial clearance and trapping in obstructive jaundice. *Ann Surg* 199:14-20, 1984.

Keller SA, Paxian M, Ashburn JH, Clemens MG, Huynh T. Kupffer cell ablation improves hepatic microcirculation after trauma and sepsis. *J Trauma* 58:740-749; 749-751, 2005.

Kennedy JA, Clements WD, Kirk SJ, McCaigue MD, Campbell GR, Erwin PJ, Halliday MI, Rowlands BJ. Characterization of the Kupffer cell response to exogenous endotoxin in a rodent model of obstructive jaundice. *Br J Surg* 86:628-633, 1999.

Kille P, Hemmings A, Lunney EA. Memories of metallothionein. *Biochim Biophys Acta* 1205:151-61, 1994.

Kimmings AN, van Deventer SJ, Obertop H, Rauws EA, Huibregtse K, Gouma DJ. Endotoxin, cytokines, and endotoxin binding proteins in obstructive jaundice and after preoperative biliary drainage. *Gut* 46:725-731, 2000.

Koeppel TA, Trauner M, Baas JC, Thies JC, Schlosser SF, Post S, Gebhard MM, Herfarth C, Boyer JL, Otto G. Extrahepatic biliary obstruction impairs microvascular perfusion and increases leukocyte adhesion in rat liver. *Hepatology* 26:1085-1091, 1997.

Kojima Y, Berger C, Vallee BL, Kägi JH. Amino-acid sequence of equine renal metallothionein-1B. *Proc Natl Acad Sci USA* 73:3413-7, 1976.

Kuebler WM, Abels C, Schuerer L, Goetz AE. Measurement of neutrophil content in brain and lung tissue by a modified myeloperoxidase assay. *Int J Microcirc* 16:89-97, 1996.

Lacaine F, Fourtanier G, Fingerhut A, Hay JM. Surgical mortality and morbidity in malignant obstructive jaundice: a prospective multivariate analysis. *Eur J Surg* 161:729-34, 1995.

Lai EC, Chu KM, Lo CY, Mok FP, Fan ST, Lo CM, Wong J. Surgery for malignant obstructive jaundice: analysis of mortality. *Surgery* 112:891-6, 1992.

Lázár G. The reticuloendothelial-blocking effect of rare earth metals in rats. *J Reticuloendothel Soc* 13:231-237, 1973.

Lázár G Jr, Husztik E, Lázár G. Effects of endotoxin and gadolinium chloride on acute septic peritonitis and septic shock in rats. *Prog Clin Biol Res* 236B:323-8, 1987.

Lázár G Jr, Paszt A, Kaszaki J, Duda E, Szakács J, Tiszlavicz L, Boros M, Balogh A, Lázár G. Kupffer cell phagocytosis blockade decreases morbidity in endotoxemic rats with obstructive jaundice. *Inflamm Res* 51:511-518, 2002.

Lawson JA, Fisher MA, Simmons CA, Farhood A, Jaeschke H. Parenchymal cell apoptosis as a signal for sinusoidal sequestration and transendothelial migration of neutrophils in murine models of endotoxin and Fas-antibody-induced liver injury. *Hepatology*. 28:761-7, 1998.

Liu J, Klaassen CD. Absorption and distribution of cadmium in metallothionein-I transgenic mice. *Fundam Appl Toxicol* 29:294-300, 1996.

Llesuy S, Evelson P, González-Flecha B, Peralta J, Carreras MC, Poderoso JJ, Boveris A. Oxidative stress in muscle and liver of rats with septic syndrome. *Free Radic Biol Med* 16:445-51, 1994.

Lorant DE, Patel KD, McIntyre TM, McEver RP, Prescott SM, Zimmerman GA. Coexpression of GMP-140 and PAF by endothelium stimulated by histamine or thrombin: a juxtacrine system for adhesion and activation of neutrophils. *J Cell Biol.* 115:223–34. 1991.

Macdonald J, Galley HF, Webster NR. Oxidative stress and gene expression in sepsis. *Br J Anaesth* 90:221-32, 2003.

Masters BA, Kelly EJ, Quaife CJ, Brinster RL, Palmiter RD. Targeted disruption of metallothionein I and II genes increases sensitivity to cadmium. *Proc Natl Acad Sci USA* 91:584-8, 1994.

Matés JM, Pérez-Gómez C, Núñez de Castro I. Antioxidant enzymes and human diseases. *Clin Biochem* 32:595-603, 1999.

McCord JM, Fridovich I. Superoxide dismutase. An enzymic function for erythrocuprein (hemocuprein). *J Biol Chem* 244:6049-55, 1969.

McCuskey RS. Hepatic microvascular response to endotoxemia and sepsis. *Prog Appl Microcirc* 19:76-84, 1993.

Michalska AE, Choo KH. Targeting and germ-line transmission of a null mutation at the metallothionein I and II loci in mouse. *Proc Natl Acad Sci USA* 90:8088-92, 1993.

Miller AM, Masrorpour M, Klaus C, Zhang JX. LPS exacerbates endothelin-1 induced activation of cytosolic phospholipase A_2 and thromboxane A_2 production from Kupffer *cells of the prefibrotic rat liver. J Hepatol 46:276-285, 2007.*

Miller SA, Dykes DD, Polesky HF. A simple salting out procedure for extracting DNA from human nucleated cells. *Nucleic Acids Res* 16:12-15, 1988.

Minter RM, Fan MH, Sun J, Niederbichler A, Ipaktchi K, Arbabi S, Hemmila MR, Remick DG, Wang SC, Su GL. Altered Kupffer cell function in biliary obstruction. *Surgery* 138:236-245, 2005.

Misra HP, Fridovich I. The role of superoxide anion in the autoxidation of epinephrine and a simple assay for superoxidedismutase. *J Biol Chem* 247:3170-3175, 1972.

Naito M, Hasegawa G, Ebe Y, Yamamoto T. Differentiation and function of Kupffer cells. Med Electron Microsc 37:16-28, 2004.

Oguro T, Takahashi Y, Ashino T, Takaki A, Shioda S, Horai R, Asano M, Sekikawa K, Iwakura Y, Yoshida T. Involvement of tumor necrosis factor alpha, rather than interleukin-1alpha/beta or nitric oxides in the heme oxygenase-1 gene expression by lipopolysaccharide in the mouse liver. *FEBS Lett* 516:63-6, 2002.

Oh HC, Lee SK, Lee TY, Kwon S, Lee SS, Seo DW, Kim MH. Analysis of percutaneous transhepatic cholangioscopy-related complications and the risk factors for those complications. *Endoscopy* 39:731-6, 2007.

O'Neil S, Hunt J, Filkins J, Gamelli R. Obstructive jaundice in rats results in exaggerated hepatic production of tumor necrosis factor-alpha and systemic and tissue tumor necrosis factor-alpha levels after endotoxin. *Surgery* 122:281-286; 1997.

Orellana M, Rodrigo R, Thielemann L, Guajardo V. Bile duct ligation and oxidative stress in the rat: effects in liver and kidney. *Comp Biochem Physiol C Toxicol Pharmacol* 126:105-11, 2000.

Padillo FJ, Cruz A, Navarrete C, Bujalance I, Briceño J, Gallardo JI, Marchal T, Caballero R, Túnez I, Muntané J, Montilla P, Pera-Madrazo C. Melatonin prevents oxidative stress and hepatocyte cell death induced by experimental cholestasis. *Free Radic Res* 38:697-704, 2004.

Pannen BH, Bauer M, Zhang JX, Robotham JL, Clemens MG. A time-dependent balance between endothelins and nitric oxide regulating portal resistance after endotoxin. *Am J Physiol* 271:H1953-1961, 1996.

Paxian M, Rensing H, Rickauer A, Schönhofen S, Schmeck J, Pannen BH, Bauer I, Bauer M. Kupffer cells and neutrophils as paracrine regulators of the heme oxygenase-1 gene in hepatocytes after hemorrhagic shock. *Shock* 15:438-45, 2001.

Pitt HA, Cameron JL, Postier RG, Gadacz TR. Factors affecting mortality in biliary tract surgery. *Am J Surg* 141:66-72, 1981.

Puntis MC, Jiang WG. Plasma cytokine levels and monocyte activation in patients with obstructive jaundice. *J Gastroenterol Hepatol* 11:7-13, 1996.

Rizzardini M, Carelli M, Cabello Porras MR, Cantoni L. Mechanisms of endotoxin-induced haem oxygenase mRNA accumulation in mouse liver: synergism by glutathione depletion and protection by N-acetylcysteine. *Biochem J* 304:477-83, 1994.

Rizzardini M, Zappone M, Villa P, Gnocchi P, Sironi M, Diomede L, Meazza C, Monshouwer M, Cantoni L. Kupffer cell depletion partially prevents hepatic heme oxygenase

1 messenger RNA accumulation in systemic inflammation in mice: role of interleukin 1beta. *Hepatology* 27:703-10, 1998.

Ruttinger D, Vollmar B, Wanner GA, Messmer K. In vivo assessment of hepatic alterations following gadolinium chloride-induced Kupffer cell blockade. *J Hepatol* 25:960-967, 1996.

Sakaguchi S, Furusawa S. Oxidative stress and septic shock: metabolic aspects of oxygen-derived free radicals generated in the liver during endotoxemia. *FEMS Immunol Med Microbiol* 47:167-77, 2006.

Sato M, Bremner I. Oxygen free radicals and metallothionein. *Free Radic Biol Med* 14:325-37, 1993.

Sauer JM, Sipes IG. Modulation of chemical-induced lung and liver toxicity by all-trans-retinol in the male Sprague-Dawley rat. *Toxicology* 105:237-49, 1995.

Serbinova E, Khwaja S, Reznick AZ, Packer L. Thioctic acid protects against ischemia-reperfusion injury in the isolated perfused Langendorff heart. *Free Radic Res Commun* 17:49-58, 1992.

Singh S, Shackleton G, Ah-Sing E, Chakraborty J, Bailey ME. Antioxidant defenses in the bile duct-ligated rat. *Gastroenterology* 103:1625-9, 1992.

Spolarics Z. Endotoxin stimulates gene expression of ROS-eliminating pathways in rat hepatic endothelial and Kupffer cells. *Am J Physiol* 270:G660-6, 1996.

Stocker R. Induction of haem oxygenase as a defence against oxidative stress. *Free Radic Res Commun* 9:101-12, 1990.

Takano H, Inoue K, Yanagisawa R, Sato M, Shimada A, Morita T, Sawada M, Nakamura K, Sanbongi C, Yoshikawa T. Protective role of metallothionein in acute lung injury induced by bacterial endotoxin. *Thorax* 59:1057-62, 2004.

Tomioka M, Iinuma H, Okinaga K. Impaired Kupffer cell function and effect of immunotherapy in obstructive jaundice. *J Surg Res* 92:276-282, 2000.

Tüzüner E, Liu L, Shimada M, Yilmaz E, Glanemann M, Settmacher U, Langrehr JM, Jonas S, Neuhaus P, Nussler AK. Heme oxygenase-1 protects human hepatocytes in vitro against warm and cold hypoxia. *J Hepatol* 41:764-72, 2004.

Van Bossuyt H, Wisse E. Cultured Kupffer cells, isolated from human and rat liver biopsies, ingest endotoxin. *J Hepatol* 7:45-56, 1988.

Vollmar B, Glasz J, Senkel A, Menger MD, Messmer K. Role of leukocytes in the initial hepatic microvascular response to endotoxemia. *Zentralbl Chir* 118:691-696, 1993.

Vollmar B, Ruttinger D, Wanner GA, Leiderer R, Menger MD. Modulation of Kupffer cell activity by gadolinium chloride in endotoxemic rats. *Shock* 6:434-441, 1996.

Xu H, Korneszczuk K, Karaa A, Lin T, Clemens MG, Zhang JX. Thromboxane A_2 from Kupffer cells contributes to the hyperresponsiveness of hepatic portal circulation to endothelin-1 in endotoxemic rats. *Am J Physiol* 288:G277-283, 2005.

Zhang JX, Jones DV, Clemens MG. Effect of activation on neutrophil-induced hepatic microvascular injury in isolated rat liver. *Shock* 1:273-278, 1994.

Zhong Z, Froh M, Wheeler MD, Smutney O, Lehmann TG, Thurman RG. Viral gene delivery of superoxide dismutase attenuates experimental cholestasis-induced liver fibrosis in the rat. *Gene Ther* 9:183-91, 2002.

Zimmerman JJ. Defining the role of oxyradicals in the pathogenesis of sepsis. *Crit Care Med* 23:616-7, 1995.

9. ANNEX